Fluid Phase Equilibria 423 (2016) 203–219

Contents lists available at ScienceDirect

Fluid Phase Equilibria

journal homepage: www.elsevier.com/locate/fluid

Multiphase isenthalpic flash integrated with stability analysis

Di Zhu, Ryosuke Okuno*

University of Texas at Austin, USA

ARTICLE INFO

Article history:
Received 12 December 2015
Received in revised form
2 April 2016
Accepted 5 April 2016
Available online 7 April 2016

Keywords:
Multiphase isenthalpic flash
Phase stability analysis
Equation of state
Narrow-boiling fluids
Compositional simulation

ABSTRACT

Isobaric, isenthalpic (PH) flash is challenging for multiphase non-isothermal flow simulation using an equation of state (EOS). This is because the number of equilibrium phases is unknown in temperature and composition space, and because the system of equations in PH flash becomes nearly degenerate for narrow-boiling fluids. The term "narrow-boiling" is used in the literature to refer to enthalpy that is sensitive to temperature.

The primary objective of this research is to develop the multiphase PH-flash algorithm integrated with stability analysis that resolves the two technical challenges mentioned above. The secondary objective is to present a new analysis of narrow-boiling behavior by coupling energy and phase behavior equations through the temperature dependency of K values. The thermodynamic model used is the Peng-Robinson EOS with the van der Waals mixing rules.

PH flash in this research is formulated by use of the tangent-plane-distance function, in which phase-split computation is integrated with phase-stability analysis. The formulated PH flash is solved by the direct-substitution algorithm with an arbitrary number of sampling compositions (N_S), at which phase stability is measured during the iteration. The number of equilibrium phases is not required to be fixed in the new algorithm.

Results in case studies show that the new algorithm can robustly handle phase appearance/disappearance with narrow-boiling behavior, including the case of one degree of freedom. The algorithm becomes more robust with increasing N_S because the possibility of finding all stationary points of the tangent-plane-distance function increases. However, the number of iterations required tends to increase with increasing N_S because the algorithm with more sampling compositions may take more iterations for merging and adding some of the sampling compositions.

The general condition presented for narrow-boiling behavior is that the interplay between energy balance and phase behavior is significant. Two subsets of the condition are derived by analyzing the convex function whose gradient vectors consist of the Rachford-Rice equations; (i) the overall composition is near an edge of composition space, and (ii) the solution conditions (temperature, pressure, and overall composition) are near a critical point, including a critical endpoint. A special case of the first specific condition is the fluids with one degree of freedom. These conditions for narrow-boiling behavior are demonstrated in case studies.

1. Introduction

Numerical solution of isothermal compositional reservoir flow has been extensively studied [1–20]. For thermal compositional reservoir flow, however, the literature is relatively scarce [21–31]. Reliable solution of the coupled equations of mass balance, energy balance, and phase behavior requires a detailed understanding of numerical difficulties that may occur in thermal compositional simulation. This paper is concerned with two major issues in isenthalpic flash for thermal compositional simulation with a cubic equation of state (EOS); one is narrow-boiling behavior and the other is phase stability analysis.

Narrow-boiling behavior refers to the total enthalpy that is sensitive to temperature [32–37]. It is related to how the energy balance affects phase behavior in thermal compositional simulation. The limiting narrow-boiling behavior occurs for fluid systems with one degree of freedom, for which the enthalpy exhibits a discontinuity in temperature space [32,33,38–40].

Various researchers reported convergence difficulties associated

* Corresponding author. Department of Petroleum and Geosystems Engineering, University of Texas at Austin, 200 E. Dean Keeton Street, Stop C0300, Austin, Texas 78712, USA.
E-mail address: okuno@utexas.edu (R. Okuno).

http://dx.doi.org/10.1016/j.fluid.2016.04.005
0378-3812/

with narrow-boiling behavior in their steam injection simulations [21,24,38,41]. The difficulties may be better handled in flow simulation with isobaric isenthalpic (PH) flash than with isobaric isothermal (PT) flash, because in the former type of thermal simulation formulation [e.g., 21, 38], narrow-boiling behavior is handled in local flash calculations that are decoupled from the global mass and energy flow equations. Even in stand-alone flash calculations, however, robust PH flash for narrow-boiling fluids has been a technical challenge [21,24,32–38]. It is not well understood under what thermodynamic conditions narrow-boiling behavior occurs; this question is addressed as one of the two main objectives in this research.

Recently, Zhu and Okuno [36,37] presented a robust direct substitution (DS) algorithm for PH flash for narrow-boiling fluids, including those with one degree of freedom. However, they did not study phase stability analysis in their PH flash. The assumption that the number of equilibrium phases is known is the major issue to be resolved for implementation of PH flash in flow simulation.

With the PH specification, the number of equilibrium phases is unknown not only in composition space, but also in temperature space. It can be determined at the solution temperature upon convergence. As presented in Brantferger [21,38], phase stability with PH specification can be analyzed only at a given temperature, which is not the equilibrium temperature until convergence.

Although phase stability analysis was not clearly described in most of the prior publications on thermal compositional simulation [e.g., 24, 29, 30, 31], it may be performed alternately with flash calculation for a fixed number of phases [21,38]. As in conventional PT flash, however, this sequential use of phase-stability and flash calculations is a series of local solutions, which requires obtaining false solutions and correcting them until the correct solution is obtained. Such PH flash becomes more difficult as the number of equilibrium phases increases because it tends to be attracted to a larger number of false solutions. It also becomes more difficult for a narrow-boiling fluid because false solutions at false temperatures may deviate substantially from the correct solution at the solution temperature for such a case.

Gupta et al. [33] proposed a novel formulation for PH flash that combines phase-stability and flash calculations. In their algorithm, the enthalpy, Rachford-Rice (RR), and stability equations were solved simultaneously for temperature, phase amounts, and stability variables. The stability variables of Gupta et al. [33] were derived from the first-order condition for unconstrained minimization of the Gibbs free energy as formulated by them. K values were updated in the outer loop based on the temperature change that was obtained from the internal iteration loop. It was reported that their algorithm could handle fluids with one degree of freedom. This is conceivable because the number of equilibrium phases is part of the solution in their PH flash [33]. To the best of our knowledge, the formulation and algorithm of Gupta et al.'s for PH flash have not been used in the literature since their original publication [33]. Various issues of their PH flash will be resolved in this paper, but briefly introduced here.

Firstly, non-convergence can occur when it attempts to solve the degenerate system of equations for a narrow-boiling fluid without using the method of Zhu and Okuno [36,37]. When narrow-boiling behavior occurs, it occurs within a phase region in which the number of phases is fixed. This is true even for the limiting case of one degree of freedom, for which the entire phase region of one freedom is narrow-boiling [e.g., a three-phase region (or point) for a binary system at a given pressure]. Thus, the coupling of phase-stability and flash calculations in itself does not necessarily improve the degeneracy issue associated with narrow-boiling behavior. Zhu and Okuno [36] presented non-convergence cases with the conventional PH flash algorithms even if the correct number of phases was used.

Secondly, it does not even start the iteration when the initial K values proposed by them yield ill-posed RR problems that have no solution. Their initial K values often form an unbounded feasible region for the RR solution. No solution exists for such a case, as proved by Okuno et al. [9].

Thirdly, their algorithm is initialized with an assumed maximum number of phases. During the iteration, if some of the phases (or iterative compositions) become close to one another, they are added together to decrease the number of iterative compositions. Subsequent computations are performed only for the distinct iterative compositions. That is, the number of iterative compositions only decreases, but does not increase, in their PH-flash algorithm. No scheme was proposed to handle the situation in which new phases appear in subsequent iterations as temperature changes in PH flash. This is problematic when the number and identities of phases change within the temperature domain of interest, as in steam injection simulation.

Fourthly, how to select a reference composition that was required to set the system of equations is unclear [33,42]. Alsaifi and Englezos [42] only stated in their paper on PT flash that a negative phase amount occurred when a reference composition was improperly selected.

Due to the various issues ranging from fundamental to implementation problems, no algorithm has been established for multiphase PH flash integrated with phase-stability analysis. In this paper, the coupling of phase-stability and flash calculations is reformulated on the basis of Brantferger's research on phase stability with PH specification [21,38]. Then, a new algorithm is presented to robustly solve the formulated multiphase PH flash. Also, a detailed analysis is given to address the unanswered question regarding thermodynamic conditions for narrow-boiling behavior. Case studies demonstrate that the developed algorithm can robustly perform multiphase PH flash integrated with phase-stability analysis even for narrow-boiling fluids, which none of the prior PH-flash algorithms [21,24,32–38] addressed in detail.

2. Formulation and algorithm

The new PH flash integrated with stability analysis is formulated by combining the conventional PH-flash formulation with the PT stability criterion that the tangent plane to the Gibbs free energy surface at a stable equilibrium state cannot lie above the Gibbs free energy surface at any composition. Then, a robust algorithm is developed for the formulated PH flash.

2.1. Formulation

The new formulation is a simple integration of the PH-flash formulation with Brantferger's analysis [21,38]. The correct phase equilibrium for a given P, $\underline{H}_{spec}$, and z_i ($i = 1, 2, \ldots, N_C$) is defined by a set of T and x_{ij} ($i = 1, 2, \ldots, N_C$, and $j = 1, 2, \ldots, N_P$) that gives the global maximum of the total entropy

$$\underline{S}^t = \sum_{j=1}^{N_P} \beta_j \underline{S}_j, \tag{1}$$

where P is pressure, $\underline{H}_{spec}$ is the specified molar enthalpy, z_i is the overall mole fraction of component i, T is temperature, x_{ij} is the mole fraction of component i in phase j, $\underline{S}^t$ is the total molar entropy, β_j is the mole fraction of phase j, $\underline{S}_j$ is the molar entropy of phase j, N_C is the number of components, and N_P is the number of equilibrium phases. The following constraints are to be satisfied:

$$z_i = \sum_{j=1}^{N_P} \beta_j x_{ij} \quad \text{for } i = 1, 2, \cdots, N_C \tag{2}$$

$$\sum_{j=1}^{N_P} \beta_j = 1.0 \tag{3}$$

$$\underline{H}_D^t - 1.0 = 0, \tag{4}$$

where $\beta_j > 0$, $\underline{H}_D^t$ is the dimensionless total molar enthalpy defined as $\underline{H}^t/\underline{H}_{spec}$, and $\underline{H}^t$ is total molar enthalpy.

Phase stability with PH specification can be analyzed at a given T, which defines the Gibbs free energy in composition space along with the specified P [21,38]. That is, the tangent plane to the Gibbs free energy surface at a stable equilibrium state at the solution T and specified P cannot lie above the Gibbs free energy surface at any composition [43,44]. Therefore, the dimensionless tangent plane distance function

$$D = \sum_{i=1}^{N_C} x_i \left(\ln x_i \varphi_i - \ln x_{iRef} \varphi_{iRef} \right) \geq 0 \tag{5}$$

for any composition x_i ($i = 1,2, \ldots N_C$) at the solution T and specified P. The fugacity coefficient of component i is denoted as φ_i. A reference equilibrium-phase composition is written as x_{iRef}. As shown in Michelsen [44], it is sufficient to check the D values at stationary points; that is,

$$D_j = \sum_{i=1}^{N_C} x_{ij} \left(\ln x_{ij} \varphi_{ij} - \ln x_{iRef} \varphi_{iRef} \right) \geq 0 \tag{6}$$

for $j = 1, 2, \ldots, N_S$. N_S is the number of stationary points of the dimensionless tangent plane distance function defined with a reference equilibrium-phase composition (x_{iRef}, where $i = 1, 2, \ldots, N_C$). Note that $N_S = N_P + N_U$, where $N_U \geq 0$ and is the number of unstable stationary points of the dimensionless tangent plane distance function. For N_P equilibrium phases, $D_j = 0$ ($j = 1, 2, \ldots, N_P$). For N_U unstable stationary points, $D_j > 0$ [$j = (N_P + 1), (N_P + 2), \ldots, N_S$].

In the above, the dimensionless tangent distance function that spans composition space is expressed as D (equation (5)), and a specific value of D at the jth stationary point is D_j (equation (6)). At a stationary point, equation (6) can be also written as

$$D_j = \ln x_{ij} \varphi_{ij} - \ln x_{iRef} \varphi_{iRef} \geq 0 \tag{7}$$

for $i = 1, 2, \ldots, N_C$. This is because the gradients of D_j in composition space are zero at a stationary point. This simplification was used in Michelsen [44].

The unified formulation for phase-stability and flash calculations in the current paper is to find a set of T and x_{ij} ($i = 1, 2, \ldots, N_C$, and $j = 1, 2, \ldots, N_S$) such that $D_j = 0$ subject to equations (2)–(4) for equilibrium phases $j = 1, 2, \ldots, N_P$, and $D_j > 0$ for unstable stationary points $j = (N_P + 1), (N_P + 2) \ldots, N_S$.

2.2. Algorithm

The solution scheme presented in this section is referred to as the multiphase isenthalpic flash algorithm integrated with stability analysis. Its main feature is the unified usage of the tangent plane distance function, D, for PH flash with adaptive selection of the reference composition for an arbitrary number of iterative compositions. A step-wise description is presented along with key equations.

Note that the formulation given in section 2.1 is based on the Gibbs free energy at the solution T and specified P. That is, equation (7) is satisfied upon convergence to the correct equilibrium solution. To avoid confusion, special attention should be given to the difference between variables in section 2.1 and iterative variables in this section.

The developed algorithm uses the tangent plane distance equations

$$f_{ij} = \ln x_{ij} \varphi_{ij} - \ln x_{ir} \varphi_{ir} - \theta_j = 0, \tag{8}$$

to update all iterative compositions x_{ij} ($i = 1, 2, \ldots, N_C$ and $j = 1, 2, \ldots, N_S$) through K values on the basis of direct substitution. Note that $\theta_j = D_j$ at an equilibrium state upon convergence. N_S is the number of sampling compositions at which phase stability is estimated during the iteration. These sampling compositions converge to stationary points; i.e., N_S becomes equal to the number of stationary points upon convergence. A reference composition is expressed as x_{ir} ($i = 1, 2, \ldots, N_C$). K values are defined as

$$K_{ij} = x_{ij} \Big/ \left(e^{\theta_j} x_{ir} \right), \tag{9}$$

for $i = 1, 2, \ldots, N_C$, $j = 1, 2, \ldots, N_S$, and $j \neq r$.

At an equilibrium state upon convergence, equation (8) becomes equation (7) (i.e., $\theta_j = D_j$), and the reference composition ($\vec{x}_r$) corresponds to one of equilibrium phases, which was denoted as x_{iRef} in equation (5). Furthermore, $D_j = 0$ for N_P equilibrium phases (i.e., $j = 1, 2, \ldots, N_P$) and $D_j > 0$ for N_U unstable stationary points [i.e., $j = (N_P + 1), (N_P + 2) \ldots, N_S$] upon convergence, where $N_S = N_P + N_U$.

During the iteration, a correct equilibrium state is searched for by updating temperature and N_S sampling compositions. The sampling compositions belong to either set P or set U. In set P, $\theta_j = 0$ and $0 < \beta_j < 1$ for $j = 1, 2, \ldots, N_P$. In set U, $\theta_j > 0$ and $\beta_j = 0$ for $j = (N_P + 1), (N_P + 2) \ldots, N_S$. Equation (8) is solved together with the material balance (equations (2) and (3)) and the enthalpy constraint, $g_{N_P} = \underline{H}_D^t - 1.0 = 0$ (equation (4)), for K values and T_D, where $T_D = T/T_{Ref}$, and T_{Ref} is some reference value that makes temperature better scaled [36,37]. The reference composition ($\vec{x}_r$) is selected from set P adaptively, as described later.

For set P, equation (9) becomes $K_{ij} = x_{ij}/x_{ir}$. The conventional RR equations give the relationship between K values and mole fractions of apparent phases (β_j's) as follows:

$$g_j = \sum_{i=1}^{N_C} (x_{ir} - x_{ij}) = \sum_{i=1}^{N_C} (1 - K_{ij}) z_i / t_i = 0 \tag{10}$$

for sampling point $j \neq r$ within set P, where $t_i = 1 - \sum_{j \neq r} (1 - K_{ij}) \beta_j$ for $i = 1, 2, \ldots, N_C$. Compositions are given as $x_{ir} = z_i/t_i$ and $x_{ij} = K_{ij} x_{ir}$ for $i = 1, 2, \ldots, N_C$.

For set U, the summation constraint $\Sigma_i x_{ij} = 1.0$ gives

$$\theta_j = -\ln \left[\sum_{i=1}^{N_C} K_{ij} x_{ir} \right] \tag{11}$$

for sampling composition j within set U. Compositions for set U are given as $x_{ij} = e^{\theta_j} K_{ij} x_{ir}$ for $i = 1, 2, \ldots, N_C$.

The algorithm presented in this section is applicable for an arbitrary number of sampling compositions, which converge to stationary points of the tangent plane distance function at an equilibrium state upon convergence. As will be presented later, sampling compositions naturally merge for a case in which N_S is greater than the number of stationary points present upon convergence.

N_S sampling compositions can be initialized by use of a correlation suitable for the fluid of interest, such as Wilson's correlation,

Li and Firoozabadi [45], and Zhu and Okuno [37], and use of certain information from the previous time-step in flow simulation. A random distribution and a distribution near vertices in composition space are useful when no reliable information is available for equilibrium phases of the fluid of interest.

The algorithm requires more sampling compositions than the number of equilibrium phases, which, in general, is unknown prior to the calculation. N_C sampling compositions may be sufficient in most petroleum applications, in which a few pseudo components are used in addition to well-defined light components, such as methane, ethane, and propane. However, at least $(N_C + 1)$ sampling compositions are required for one degree of freedom for multi-component mixtures. In general, the iterative solution with this algorithm becomes more robust as N_S increases, because more information about the Gibbs free energy is carried by more sampling compositions. However, use of more sampling compositions lowers the computational efficiency, as will be shown in the case studies. With N_S less than N_C, the algorithm may fail to find the correct number of equilibrium phases, unless specific information about equilibrium phases is available prior to the calculation.

The fundamental structure of the current algorithm broadly follows the direct substitution algorithm developed by Michelsen [34], but is newly designed for integrated flash-stability calculations on the basis of the PH-flash algorithm developed by Zhu and Okuno [37]. Each iteration first solves equations (10) and (11) for sets P and U, respectively, in sequence for a given set of K values and overall composition. Then, the traditional direct substitution with equation (8) updates K values for sets P and U in composition space. After that, one Newton's iteration step is performed for $(N_P - 1)$ β's and T_D by use of the system of N_P equations (equations (4) and (10)), as in Michelsen [34]. Finally, K values for sets P and U are updated in temperature space for the subsequent iteration.

This fundamental structure is augmented by various important steps for robustness. As mentioned in Section 1, for example, it is crucial to check the feasibility for each RR solution by use of the method of Okuno et al. [9]. The constraint, $a_i^T\boldsymbol{\beta} \le b_i$, where $a_i = \{1 - K_{ij}\}$, $\boldsymbol{\beta} = \{\beta_j\}$, $b_i = \min\{1 - z_i, \min_j\{1 - K_{ij}z_i\}\}$, is to be satisfied if there exists a bounded feasible region for each RR solution [9]. Also, the decoupling of T_D from β's is necessary to solve degenerate systems of equations (equations (4) and (10)) for narrow-boiling fluids, as presented in Zhu and Okuno [36,37]. A new analysis of narrow-boiling behavior will be presented in the next section. Furthermore, the upper and lower temperature limits (T_D^U and T_D^L) are used not to have unrealistic temperature values during the iterations. In this research, the upper and lower temperature limits are selected at 288.15 K and 775 K, respectively. The limits are set to cover a sufficiently wide range of temperatures for the application of interest. The initial guess for temperature should be within the limits.

The Peng-Robinson (PR) EOS [46,47] with the van der Waals mixing rules is used to calculate thermodynamic properties in this research. Pertinent derivatives can be found in Zhu and Okuno [36]. A stepwise description of the multiphase isenthalpic flash algorithm integrated with stability analysis is given below. The flow chart of the algorithm presented in this section is given in **Appendix A**.

Step 1. Specify $\underline{H}_{spec}$, P, and overall composition $\vec{z}$, along with model parameters, such as critical temperature T_C, critical pressure P_C, acentric factor ω, and $N_C \times N_C$ binary interaction parameters (BIPs). Input an initial guess for dimensionless temperature, $T_D^{(1)}$, where the number in the bracket represents the iteration-step number $k = 1$.

Step 2. Set N_S sampling compositions $\vec{x}_j^{(k)}$ for $j = 1, 2, \ldots, N_S$.

Step 3. Calculate D_j (equation (6)) with $\vec{z}$ as the reference composition for $j = 1, 2, \ldots, N_S$. Select the sampling composition that has the minimum D value as the reference composition $\vec{x}_r^{(k)}$. Calculate K values, $\vec{K}_j^{(k)}$, by use of $\ln K_{ij} = \ln\varphi_{ir} - \ln\varphi_{ij}$ for $j = 1, 2, \ldots, N_S$ and $j \neq r$, which is derived from equations (8) and (9). Recalculate D_j with the selected reference composition. Set N_U as the number of sampling compositions that have positive D values. $N_P = N_S - N_U$. If $N_P = 1$, go to step 7. Otherwise, go to step 4.

Step 4. Check to see if the feasible region for the RR equations (set P) is bounded [9]. If so, go to step 6. Otherwise, go to step 5.

Step 5. Exclude from set P as many sampling compositions as required until the feasibility is satisfied for the given RR problem. The exclusion is conducted in the descending order in terms of D within set P. Then, update N_P. If $N_P = 1$, go to step 7. Otherwise, continue to step 6.

Step 6. Solve the RR equations (equation (10)) for set P to obtain $\beta_j^{(k)}$ and $\vec{x}_j^{(k)}$ for $j = 1, 2, \ldots, N_P$.

Step 7. Calculate $\theta_j^{(k)}$ and $\vec{x}_j^{(k)}$ for set U, where $j = (N_P + 1), (N_P + 2) \ldots, N_S$, by use of equation (11).

Step 8. If $\theta_j^{(k)} > 0$ for $j = (N_P + 1), (N_P + 2) \ldots, N_S$, go to step 9. Otherwise, set $\theta_j^{(k)} = 0$, and select the sampling composition that has the minimum θ_j value, as the reference composition. Then, update N_P and K values with the new reference composition. Go to step 11.

Step 9. If $0 < \beta_j^{(k)} < 1$ for $j = 1, 2, \ldots, N_P$, go to step 10. Otherwise, set $\beta_j^{(k)} = 0$ and $\theta_j^{(k)} \neq 0$, and select the sampling composition with $0 < \beta_j < 1$ as the reference composition. Then, update N_P and K values with the new reference composition. Go to step 11.

Step 10. Stop, if $\left\| \vec{f}_j^{(k)} \right\|_\infty < \varepsilon_f$ (e.g., $\varepsilon_f = 10^{-10}$) and $|g_{NP}^{(k)}| < \varepsilon_h$ (e.g., $\varepsilon_h = 10^{-10}$) for $j = 1, 2, \ldots, N_S$ $(r \neq j)$. Otherwise, go to step 11.

Step 11. Check for merging compositions. If $\left\| \vec{x}_j^{(k)} - \vec{x}_q^{(k)} \right\|_\infty < \varepsilon_x$ (e.g., $\varepsilon_x = 10^{-3}$) for $j, q = 1, 2, \ldots, N_S$, and $j \neq q$, delete the jth sampling composition. Add a new sampling composition, and update the reference composition. Then, go to step 12.

Step 12. Update K values in composition space for sets P and U by use of $\ln K_{ij} = \ln\varphi_{ir} - \ln\varphi_{ij}$ for $j = 1, 2, \ldots, N_S$ and $j \neq r$. If $N_P = 1$, go to step 7. Otherwise, go to step 13.

Step 13. Construct the $N_P \times N_P$ Jacobian matrix only for set P, and calculate its condition number. If the condition number is greater than ξ (e.g., 10^6), go to step 16. Otherwise, perform one Newton's iteration step to obtain $\beta_j^{(k+1)}$ and $T_D^{(k+1)}$ for $j = 1, 2, \ldots, N_P$.

Step 14. Check to see if $T_D^L < T_D^{(k+1)} < T_D^U$. If so, continue to step 15. Otherwise, update $T_D^{(k+1)}$ using the Regula Falsi method [37].

Step 15. Update K values in temperature space for sets P and U: $\ln K_{ij}^{(k+1)} = \ln K_{ij}^{(k)} + [T_D^{(k)}(T_D^{(k+1)} - T_D^{(k)})/T_D^{(k+1)}](\partial \ln K_{ij}/\partial T_D)^{(k)}$. Go to step 4 after increasing the iteration-step number by one: $k = k + 1$.

Step 16-1. Set t_L to the highest temperature between T_D^L and $T_D^{(k)}$ that gives a negative g_{NP}. Set t_U to the lowest temperature between T_D^U and $T_D^{(k)}$ that gives a positive g_{NP}.

Step 16-2. $T_D^{(k+1)} = 0.5(t_L + t_U)$.

Step 16-3. Perform PT flash at $T_D^{(k+1)}$ to calculate $\beta_j^{(k+1)}$, $\theta_j^{(k+1)}$ and $\vec{x}_j^{(k+1)}$ such that $\left\| \vec{f}_j^{(k+1)} \right\|_\infty < \varepsilon_f$ for $j = 1, 2, \ldots, N_S$, and $r \neq j$.

Step 16-4. Calculate the condition number of the Jacobian matrix. If it is greater than ξ, continue to step 16-5. Otherwise, go to step 4.

Step 16-5. Calculate $g_{NP}^{(k+1)}$. If $|g_{NP}^{(k+1)}|$ is less than ε_h, stop. Otherwise, $t_L = T_D^{(k+1)}$ for $g_{NP}^{(k+1)} < 0$, and $t_U = T_D^{(k+1)}$

Table 1
Properties for the ternary mixture (case 1). The critical properties of water were taken from Ref. [51].

Component	Mole fraction	T_C, K	P_C, bar	ω	C^0_{P1}, J/(mol·K)	C^0_{P2}, J/(mol·K^2)	C^0_{P3}, J/(mol·K^3)	C^0_{P4}, J/(mol·K^4)
Water	0.022	672.48	277.15	0.2699	32.200	1.907×10^{-3}	1.055×10^{-5}	-3.596×10^{-9}
C_4	0.928	421.56	36.01	0.2127	9.490	3.313×10^{-1}	-1.108×10^{-4}	-2.822×10^{-9}
C_B	0.050	847.17	10.64	1.0406	−31.900	3.612	-2.044×10^{-3}	4.486×10^{-7}

Binary interaction parameters:

	Water	C_4	C_B
Water	0.0000	0.5602	0.1100
C_4	0.5602	0.0000	0.0750
C_B	0.1100	0.0750	0.0000

for $g_{NP}^{(k+1)} > 0$. Then, go to step 16-2 after increasing the iteration-step number by one; k = k + 1.

In Step 3, a reference composition is initialized to define equation (8). First, function D (equation (5)) with the overall composition as the reference is used to calculate D_j (equation (6)) at N_S sampling compositions (j = 1,2, …,N_S). Then, the initial reference composition is defined at which D is the minimum among the N_S sampling compositions. This procedure is also used when a new reference composition is to be selected during the iterations. Note that D values are used only for the initialization of sampling compositions.

In Step 11, the sampling composition to be added is taken from the previous iteration in this research. The composition that has a greater distance from that of the merged sampling composition is added. The purpose of adding a sampling composition in step 11 is to keep the original Ns, which should be always equal to or greater than the number of stationary points on the tangent plane distance function. It has been observed that this step is crucial for PH flash for water/solvent/bitumen mixtures, in which the number and identities of phases can change frequently with temperature for a given overall composition and pressure.

The algorithm presented in this paper is substantially different from that of Gupta et al. [33]. An important difference comes from the difference in formulation; that is, they introduced an additional set of equations, $\beta_j\theta_j/(\beta_j + \theta_j) = 0$, which were called "stability equations" in their papers. These additional equations were solved simultaneously with equations (4) and (10) in their algorithm. However, the unified formulation presented earlier in this section clearly shows that the complete formulation does not require Gupta et al.'s stability equations. Consequently, the Jacobian matrix in step 13 is always smaller than that of Gupta et al. which is of $(2N_P - 1) \times (2N_P - 1)$.

A second difference is in the initialization step. Gupta et al. [33] proposed their own initialization scheme for estimation of K values. Their initialization scheme excludes the sampling compositions that have positive D values from equation (5) with the overall composition as the reference composition. This often leads to non-convergence due to an unbounded feasible region for the RR solution, as described in Okuno et al. [9]. A third difference is that the algorithm of Gupta et al. [33] uses Newton's iteration step even for a narrow-boiling fluid, for which the system of equations is nearly degenerate [36,37]. This leads to non-convergence as studied in detail by Zhu and Okuno [36,37]. The algorithm in this research adaptively switches between Newton's iteration and bisection depending on the condition number of the Jacobian matrix. A fourth difference is in the selection of a reference composition $\vec{x}_r$. Although it is not clear in Gupta et al. [33], improper selection of a reference phase was found by negative phase amounts in Alsaifi and Englezos [42]. The selection of $\vec{x}_r$ given in steps 3, 8, and 9 is based on the fundamental principle that the lowest Gibbs free energy should be searched for in composition space, as presented earlier in this section. A fifth difference lies in the stopping criteria. In this research, the fugacity and enthalpy equations are properly satisfied upon convergence. This is in contrast to the algorithm of Gupta et al. [33], which tests only the difference between two consecutive iteration steps in terms of temperature and phase compositions.

3. Analysis of narrow-boiling behavior

In this section, the thermodynamic conditions for narrow-

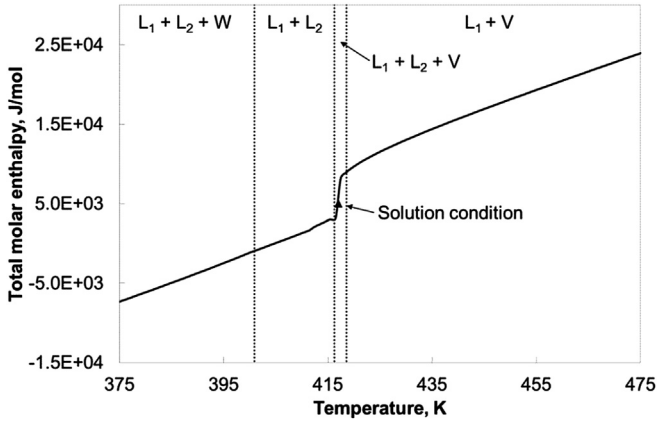

Fig. 1. Total molar enthalpy at 35 bars for the ternary mixture given in Table 1. At 35 bars, C_B-rich phase (L_1) + C_4-rich phase (L_2) + aqueous phase (W) exists from 375 K to 400.89 K, $L_1 + L_2$ from 400.89 K to 416.24 K, $L_1 + L_2$ + vapor phase (V) from 416.24 K to 418.55 K, and $L_1 + V$ from 418.55 K to 475 K. $\underline{H}^t$ is highly non-linear with respect to temperature near phase transition from $L_1 + L_2$ to $L_1 + L_2 + V$.

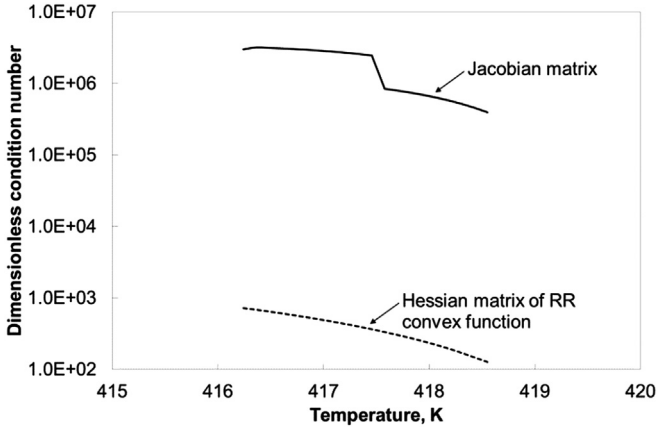

Fig. 2. Dimensionless condition number of Jacobian matrix and the Hessian matrix of the RR convex function (equation (13)) in $L_1 + L_2 + V$ region at 35 bars for the ternary mixture given in Table 1. The scaling of temperature and enthalpy is conducted with T_{ref} of 300 K and $\underline{H}_{spec}$ of 5000 J/mol. The dimensionless Jacobian condition number exceeds 10^6 between 416.24 K and 417.55 K. The Hessian matrix is reasonably well-conditioned; hence, the RR portion of the system of equations is not problematic in the three-phase region.

Table 2a
Six sampling compositions at the 1st iteration (case 1).

	Composition 1	Composition 2	Composition 3	Composition 4	Composition 5	Composition 6
x_{ij}	$5.011728395 \times 10^{-2}$	$5.000000000 \times 10^{-4}$	$5.000000000 \times 10^{-4}$	$2.024691358 \times 10^{-1}$	$2.026337137 \times 10^{-1}$	$9.990000000 \times 10^{-1}$
	$8.484938271 \times 10^{-1}$	$9.990000000 \times 10^{-1}$	$5.000000000 \times 10^{-4}$	$6.906419752 \times 10^{-1}$	$4.016934042 \times 10^{-1}$	$5.000000000 \times 10^{-4}$
	$1.013883334 \times 10^{-1}$	$5.000000000 \times 10^{-4}$	$9.990000000 \times 10^{-1}$	$1.068888890 \times 10^{-1}$	$3.956728821 \times 10^{-1}$	$5.000000000 \times 10^{-4}$

Table 2b
Six sampling compositions at the 2nd iteration before the merging of compositions 2 and 4 (case 1).

	Composition 1	Composition 2	Composition 3	Composition 4	Composition 5	Composition 6
x_{ij}	$9.999996463 \times 10^{-1}$	$1.048995656 \times 10^{-2}$	$1.033333973 \times 10^{-2}$	$1.051640199 \times 10^{-2}$	$9.013291891 \times 10^{-3}$	$8.932510699 \times 10^{-3}$
	$3.536746148 \times 10^{-7}$	$9.767356013 \times 10^{-1}$	$9.753538516 \times 10^{-1}$	$9.767748394 \times 10^{-1}$	$9.444418053 \times 10^{-1}$	$9.413768141 \times 10^{-1}$
	$2.538515500 \times 10^{-11}$	$1.277444214 \times 10^{-2}$	$1.431284427 \times 10^{-2}$	$1.270875861 \times 10^{-2}$	$4.654490280 \times 10^{-2}$	$4.969067520 \times 10^{-2}$

boiling behavior are investigated on the basis of the PR EOS. The term "narrow-boiling" has been used in the literature to indicate the enthalpy behavior that is substantially sensitive to temperature. Narrow-boiling behavior occurs as a result of the significant interplay between the energy balance and phase behavior equations, as explained below.

Zhu and Okuno [36,37] concluded that narrow-boiling behavior occurs when at least one of the phase compositions (x_{ij} for $i = 1, 2, \ldots, N_C$ and $j = 1, 2, \ldots, N_P$) drastically changes with a small change in temperature so that phase mole fractions (β_j for $j = 1, 2, \ldots, N_P$) significantly change. That is, it is related directly to the sensitivity of K values to temperature. Therefore, narrow-boiling behavior can be effectively analyzed on the basis of the equations (4) and (10) that are coupled through the temperature dependency of K values as presented in Zhu and Okuno [48]. Note that the analysis presented in this section only includes equilibrium phases; i.e., $\overrightarrow{x}_j$ for $j = 1, 2, \ldots, N_P$.

Appendix B gives the analytical expressions of each element in the $N_P \times N_P$ Jacobian matrix for a N_C-component N_P-phase system. The Jacobian matrix is formed by dimensionless equations (4) and (10) with respect to independent β_j and T_D. The major block of $(N_P - 1) \times (N_P - 1)$ in the Jacobian matrix comes from the RR equations with respect to independent β's. This part corresponds to the Hessian matrix of the convex function that was used by Okuno et al. [9] to solve RR as a convex minimization problem in multiphase compositional reservoir simulation. Appendix B shows that if the total enthalpy becomes sensitive to temperature (i.e., narrow-boiling behavior, or $\partial g_{NP}/\partial T_D$ becomes large), the Jacobian tends to be ill-conditioned regardless of the curvature of the RR convex function. This is consistent with the cases shown in Zhu and Okuno [36], and also can be understood from the following equation;

$$\underline{H}_D^t = \sum_{j=1}^{N_P} \beta_j \underline{H}_{Dj}, \tag{12}$$

where $\underline{H}_{Dj}$ is the dimensionless molar phase enthalpy. Equation (12) shows that the total enthalpy becomes sensitive to temperature if a small temperature change causes K values to drastically change so that the RR solution gives substantially different β's between the two temperatures.

More specific conditions for narrow-boiling behavior can be derived on the basis of the analysis of a convex function whose gradient vectors consist of the RR equations as follows. Okuno et al. [9] presented a non-monotonic convex function whose gradient vectors consist of the RR equations as

$$F(\boldsymbol{\beta}) = \sum_{i=1}^{N_C} (-z_i \ln |t_i|), \tag{13}$$

where $\boldsymbol{\beta}$ is the vector of independent mole fractions [i.e., β_j for $j = 1, 2, \ldots, (N_P - 1)$]. A derivation of the function can be found in Okuno et al. [9]. The convex function in Okuno et al. [9] is similar to the ones presented in Michelsen [49] and Leibovici and Nichita [50]. Multiphase RR equations can be correctly solved by the following formulation:

$$\text{Minimize } F(\boldsymbol{\beta}) = \sum_{i=1}^{N_C} (-z_i \ln |t_i|) \text{ subject to } a_i^T \boldsymbol{\beta} \le b_i, \tag{14}$$

where $a_i = \{1 - K_{ij}\}$, and $b_i = \min\{1 - z_i, \min_j\{1 - K_{ij} z_i\}\}$ for $i = 1, 2, \ldots, N_C$, and $j = 1, 2, \ldots, (N_P - 1)$ [9]. The feasible region was derived on the basis of the non-negativity of phase component mole fractions, $0 \le x_{ij} \le 1$ for $i = 1, 2, \ldots, N_C$, and $j = 1, 2, \ldots, N_P$ [9].

The Hessian matrix of $(N_P - 1) \times (N_P - 1)$ for the minimization is

$$\nabla^2 F = \left\{H_{kj}\right\} = \left\{Y^T D Y\right\}, \tag{15}$$

where $H_{kj} = \sum_{i=1}^{N_C} [(1 - K_{ij})(1 - K_{ik}) z_i] / t_i^2$, $D = \text{diag}(z_1, \ldots, z_{N_C}) \in \mathbb{R}^{N_C \times N_C}$, and $Y = \{Y_{ij}\} = \{(1 - K_{ij})/t_i\} \in \mathbb{R}^{N_C \times (N_P - 1)}$. The D matrix is positive definite because z_i ($i = 1, 2, \ldots, N_C$) are all positive (i.e., positive composition space). The Hessian matrix is only positive semi-definite if Y is not of full rank; i.e., at critical points, including critical endpoints where two of three equilibrium phases merge in the presence of the other non-critical phase. In such cases, there exists a direction along which F is constant as proved by Okuno et al. [9]. No solution exists in the minimization for such cases.

If the D matrix is not positive definite (in negative composition space), the positive definiteness of the Hessian matrix is not guaranteed even if Y is of full rank. Negative z_i values do not occur in practical simulations, but were considered here to indicate the limiting behavior of the Hessian matrix in composition space.

In summary, the degree of positive definiteness of the Hessian

Table 2c
Six sampling compositions at the 63rd iteration (case 1).

	Composition 1	Composition 2	Composition 3	Composition 4	Composition 5	Composition 6
x_{ij}	$9.963029187 \times 10^{-1}$	$3.987093567 \times 10^{-2}$	$4.042558722 \times 10^{-2}$	$2.821421577 \times 10^{-2}$	$2.844511013 \times 10^{-2}$	$1.762505600 \times 10^{-2}$
	$1.753511927 \times 10^{-11}$	$9.599949394 \times 10^{-1}$	$9.517664807 \times 10^{-1}$	$7.764909338 \times 10^{-1}$	$8.109556208 \times 10^{-1}$	$9.629795682 \times 10^{-1}$
	$3.697081246 \times 10^{-3}$	$1.341248777 \times 10^{-4}$	$7.807932011 \times 10^{-3}$	$1.952948503 \times 10^{-1}$	$1.605992690 \times 10^{-1}$	$1.939537572 \times 10^{-2}$

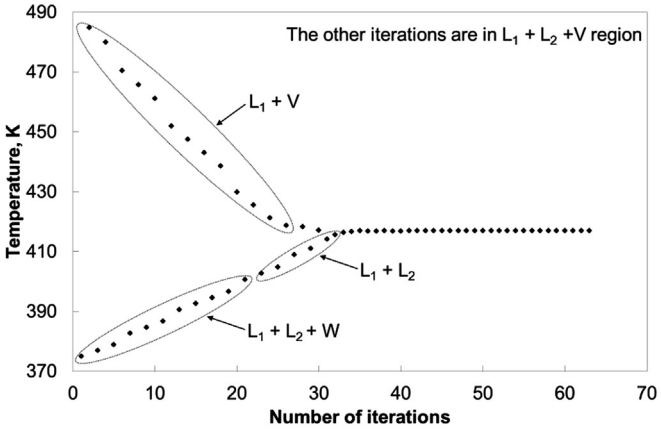

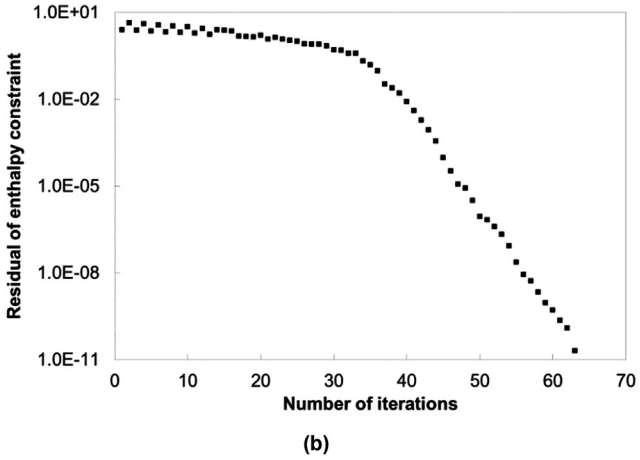

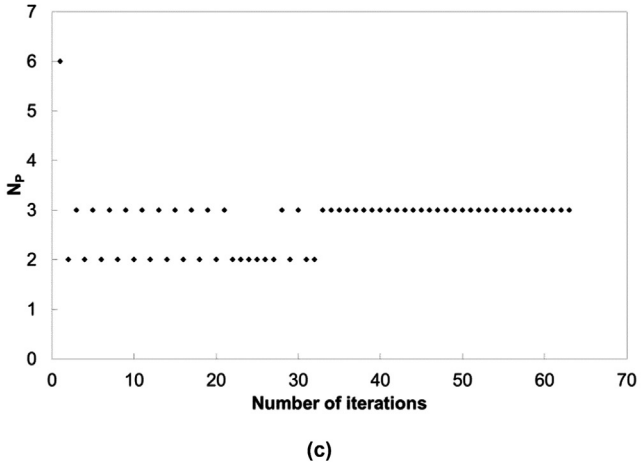

Fig. 3. Convergence behavior of the current algorithm for the ternary mixture given in Table 1 at 35 bars and 5000 J/mol: (a) T, (b) residual of equation 4, and (c) N_P. The initial T is set to 375 K, where $L_1 + L_2 + W$ coexist. In this calculation, N_S is set to six, of which three sampling points are placed near compositional vertices. The other three sampling compositions are randomly distributed (see Table 2a). The solution temperature is 416.89 K, where narrow-boiling behavior occurs (see Fig. 1).

matrix tends to become lower as the overall composition becomes closer to an edge of positive composition space (e.g., at least one component is of nearly-zero concentration) and/or the solution conditions (temperature, pressure, overall composition) become closer to a critical point. The solution of the minimization for such cases tends to be sensitive to the K values used, because of small gradients of the convex function. This leads to narrow-boiling behavior. This can be easily confirmed by plotting the RR convex function for two phases near a critical point or near the vertex of a component with a K value close to unity in positive composition space, for example.

Appendix B shows that the system of equations are degenerate if the Hessian matrix is semi-positive definite. Therefore, the following are conditions that can cause narrow-boiling behavior: (i) the overall composition is near an edge of positive composition space, and (ii) the solution conditions (temperature, pressure, and overall composition) are near a critical point, including a critical endpoint.

These conditions are qualitative unless a quantitative definition is given for narrow-boiling behavior. Therefore, the degeneracy level of the system of equations is quantified on the basis of the condition number of the Jacobian matrix in this research, as in Zhu and Okuno [36] (see Appendix B for the Jacobian matrix). The condition number of 10^6 is used to detect narrow-boiling behavior in computations with the double-precision floating-point numbers (see Step 13 in the previous section).

The two conditions mentioned above are contained by the general condition for narrow-boiling behavior that K values are sensitive to temperature. Although the two specific conditions are qualitative, the analysis of the RR convex function gives the clear limiting conditions towards which the tendency of narrow-boiling behavior increases. For instance, the RR problem is uniquely defined only for $N_C \geq N_P$ (i.e., more than one degree of freedom). For one degree of freedom (e.g., three phases for a binary system), K values discontinuously changes at the temperature of interest, which causes the limiting narrow-boiling behavior as an exact discontinuity of enthalpy with respect to temperature. This is a special case of the first condition mentioned previously in this section.

4. Case studies

In this section, the algorithm developed in this research is applied to three different mixtures, which exhibit narrow-boiling behavior. One case has only one degree of freedom, which is the limiting case of narrow-boiling behavior. Different reasons for the narrow-boiling behavior in the cases are explained based on the analysis given in the previous section. The mixtures used in this section present three phases at most. Although not shown in this paper, the algorithm has been successfully tested also for the four-phase case given in Zhu and Okuno [37]. The only possible comparison is made with the algorithm of Gupta et al. [33], for which various issues were discussed previously in this paper. They are highlighted in case 1 given below.

Sampling compositions are initialized by use of a random distribution and a distribution near vertices in composition space, unless otherwise stated. That is, when $N_S = N_C$, the N_S compositions are placed near the N_C vertices in composition space. When $N_S > N_C$, N_C sampling compositions are placed near the compositional vertices, and the other $(N_S - N_C)$ sampling compositions are distributed by use of a random-number generator. A sampling composition selected near a compositional vertex consists of 99.9% that component and 0.1% the equimolar mixture of the other components in this section.

4.1. Case 1

Case 1 uses three components consisting of 2.2% water (w), 92.8% n-butane (C_4), and 5.0% bitumen (C_B). The components' properties are given in Table 1. The critical properties for water were taken from Ref. [51]. They are not physical values, but were optimized in terms of vapor pressure and density using the PR EOS. This mixture is used because it gives complicated phase behavior

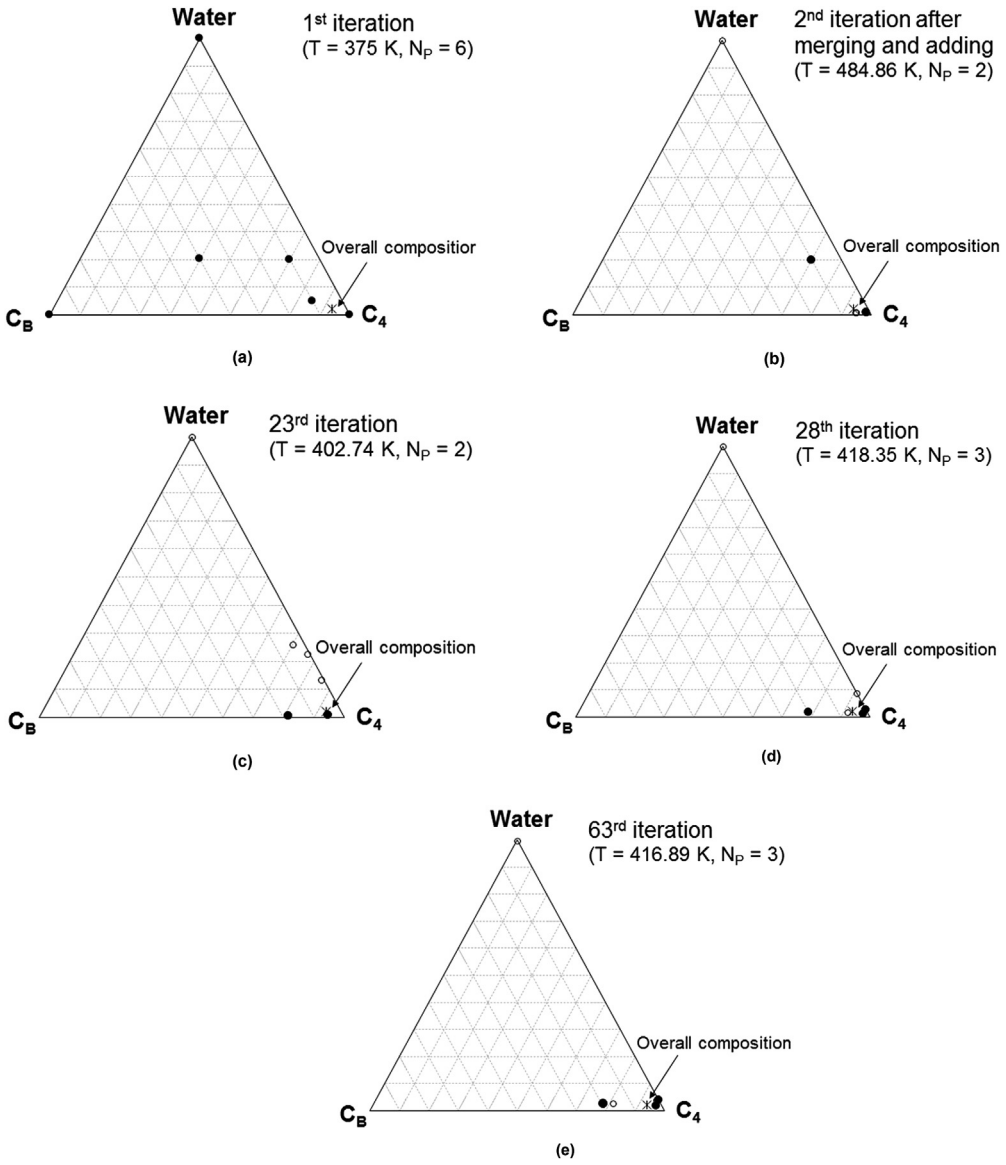

Fig. 4. Ternary diagrams at 35 bars for the ternary mixture given in Table 1 at different iteration steps. In these ternary diagrams, solid dots represent the sampling compositions in set P, which are considered for material balance. Hollow dots represent the sampling compositions in set U, which are excluded from material balance. (a) Ternary diagram at the 1st iteration where L_1, L_2, and W coexist (T = 375 K). (b) Ternary diagram point at the 2nd iteration where L_1 and V coexist (T = 484.86 K) after merging, adding and re-selecting reference. (c) Ternary diagram at the 23rd iteration where L_1 and L_2 coexist (T = 402.74 K). (d) Ternary diagram at the 28th iteration where L_1, L_2, and V coexist (T = 418.35 K). (e) Ternary diagram at the 63rd iteration where L_1, L_2, and V coexist (T = 416.89 K).

and serves as a challenging case for the algorithm developed in this research. Whether this phase behavior occurs in reality is uncertain and beyond the scope of this research.

Fig. 1 shows $\underline{H}^t$ from 375 K to 475 K at 35 bars. At 35 bars, C_B-rich phase (L_1) + C_4-rich phase (L_2) + aqueous phase (W) exists from 375 K to 400.89 K, $L_1 + L_2$ from 400.89 K to 416.24 K, $L_1 + L_2$ + vapor phase (V) from 416.24 K to 418.55 K, and $L_1 + V$ from 418.55 K to 475 K. $\underline{H}^t$ is highly non-linear with respect to temperature near the phase transition between $L_1 + L_2$ and $L_1 + L_2 + V$.

Fig. 2 shows the Jacobian condition number in the $L_1 + L_2 + V$ region at 35 bars. The scaling of temperature and enthalpy is conducted with T_{ref} of 300 K and $\underline{H}_{spec}$ of 5000 J/mol. The Jacobian condition number exceeds 10^6 between 416.24 K and 417.55 K, indicating narrow-boiling behavior. Fig. 2 also show that the Hessian matrix of the RR convex function (equation (13)) is reasonably well-conditioned; hence, the RR portion of the system of equations is not problematic in the three-phase region. However, Fig. 1 clearly shows that the total enthalpy is sensitive to temperature near the phase boundary between $L_1 + L_2$ and $L_1 + L_2 + V$. In this case, therefore, the narrow-boiling behavior occurs because K values are sensitive to temperature.

A PH flash calculation at 35 bars and 5000 J/mol is considered for this ternary fluid. The initial T is set to 375 K, at which $L_1 + L_2 + W$ coexist. In this calculation, N_S is set to six, of which three sampling compositions are placed near the compositional vertices. The other three sampling compositions are randomly distributed (see Table 2a). The solution temperature is 416.89 K in the narrow-boiling region (see Fig. 1).

Fig. 3 shows the iterative solution in terms of T, residual of equation (4) (g_{NP}), and N_P. At the 30th iteration when T is 417.10 K, narrow-boiling behavior is detected by a large condition number of the Jacobian matrix. From this iteration on, T_D is decoupled from β's until it linearly converges to the correct solution at the 63rd iteration. The iterative temperature fluctuates between different phase

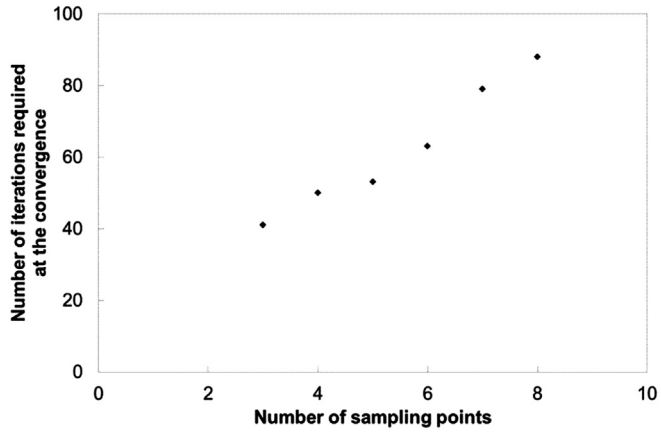

Fig. 5. Number of iterations required for convergence increases with the number of sampling points used. This is the PH flash for the ternary mixture given in Table 1 at 35 bars and 5000 J/mol. All calculations start at the same initial T (375 K). The three sampling points that are always used are near the compositional vertices. The other sampling compositions are randomly distributed for $N_S > 3$. The proposed algorithm successfully converges to the correct solution as long as N_S is greater than two.

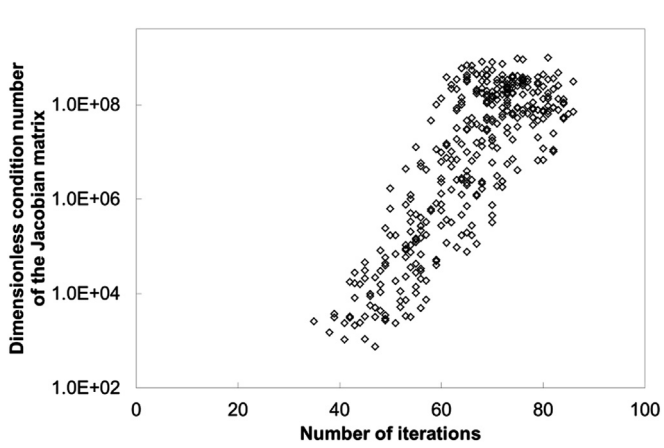

Fig. 6. Dimensionless Jacobian condition number with respect to the number of iterations required for convergence for the ternary mixture given in Table 1. Among the 350 discrete PH specifications, 240 PH conditions lie in the narrow-boiling region. All calculations start at the same initial T, 375 K, using three sampling compositions near the compositional vertices. Results show that number of iterations required increases with the condition number of Jacobian matrix.

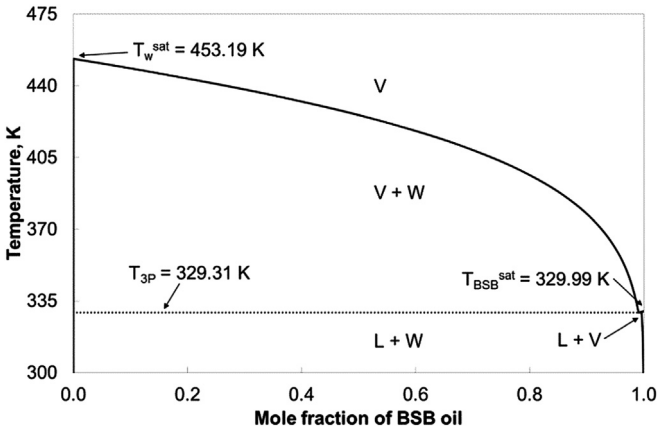

Fig. 7. T-x cross section for 99% water and 1% BSB oil at 10 bars on the basis of the PR EOS. The components' properties are given in Table 3. Three equilibrium phases, L, V, and W, are calculated to coexist at 329.31 K (T_{3P}). A discontinuity of two-phase K values occurs at T_{3P}. Also, K values in the V + W region rapidly change with temperature.

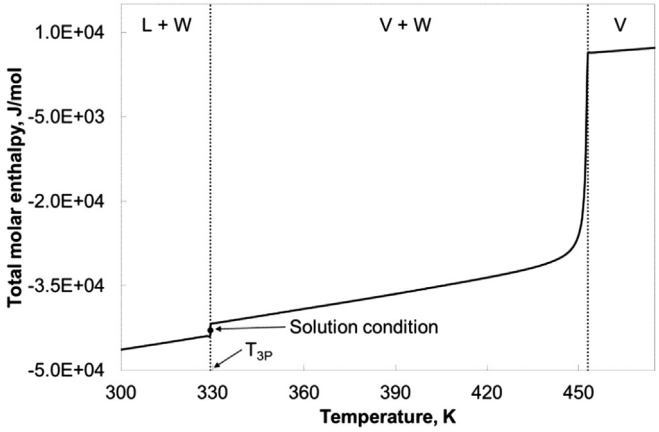

Fig. 8. Total molar enthalpy for 99% water and 1% BSB oil at 10 bars. The components' properties are given in Table 3. $\underline{H}^t$ is substantially nonlinear with respect to temperature. It is discontinuous at T_{3P}.

regions, indicating the complex solution (Fig. 3a). As shown in Fig. 3c, N_P also fluctuates until the correct number of phases is detected at the 33rd iteration. Two sampling compositions merge at the 2nd iteration in this case. However, N_S remains six during the iteration, because a new sampling point is added once the merging occurs as described in the algorithm section.

Fig. 4 shows the six sampling compositions at different iteration steps. In these ternary diagrams, solid dots represent the sampling compositions in set P, which are considered for material balance. Hollow dots represent the sampling compositions in set U, which are excluded from material balance. The 1st iteration starts with all sampling compositions included in material balance in this case. Therefore, the initial β's are calculated through the conventional RR equations (equation (10)), and the θ's are zero.

At the 2nd iteration, two sampling compositions merge. Table 2b shows the compositions of sampling points at the 2nd iteration before the merging. Sampling compositions 2 and 4 are merged. Sampling composition 4 is deleted. Then, a new sampling composition is added in order to maintain N_S of six. The new sampling composition is selected from the previous iteration step, which is the one that has a greater difference from the deleted sampling composition. Then, sampling composition 4 is replaced by (0.2025, 0.6906, 0.1069). After that, only sampling compositions 4 and 6 are included in material balance, as shown by the two solid dots in Fig. 4b. Fig. 4c and d shows the sampling compositions at the 23rd and 28th iterations, in which the iterative temperatures lie in different phase regions as shown in Fig. 3a. Fig. 4e shows the sampling compositions at the 63rd iteration, in which three equilibrium compositions are obtained. The final set of sampling

Table 3
Properties of the binary mixture consisting of 99% water (w) and 1% Bob Slaughter Block (BSB) oil (case 2).

Component	Mole fraction	MW g/mol	T_C K	P_C bar	ω	C_{P1}^0 J/(mol·K)	C_{P2}^0 J/(mol·K^2)	C_{P3}^0 J/(mol·K^3)	C_{P4}^0 J/(mol·K^4)
Water	0.99	18.015	647.300	220.890	0.344	32.20	1.907×10^{-3}	1.055×10^{-5}	-3.596×10^{-9}
BSB oil	0.01	118.834	335.089	11.224	0.392	−13.28	1.607	-8.971×10^{-4}	6.581×10^{-11}

Binary interaction parameter for water with the BSB oil is 0.525.

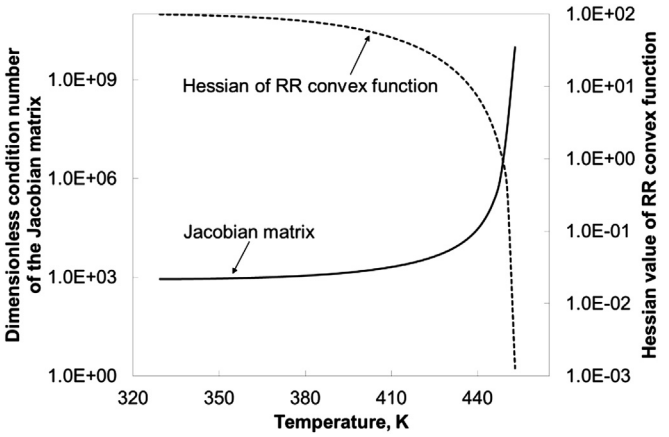

Fig. 9. Dimensionless condition number of Jacobian matrix and the Hessian matrix of the RR convex function (equation (13)) within the V + W region at 10 bars for 99% water and 1% BSB oil at 10 bars. The components' properties are given in Table 3. Note that the Hessian matrix for two-phase RR is of 1 × 1 (i.e., a scalar). T_{ref} of 300 K and $\underline{H}_{spec}$ of −5000 J/mol are used to calculate T_D and $\underline{H}^t_D$. Narrow-boiling behavior occurs for temperature above 447.73 K using the criterion that the condition number of the Jacobian matrix with dimensionless variables is greater than 10^6. It is evident from the figure that the convexity of the RR convex function is substantially reduced in the narrow-boiling region, which verifies the analysis given in the previous section.

compositions is presented in Table 2c. The three equilibrium phases are compositions 2, 4, and 6. The θ values at the other three compositions are positive, indicating that they are unstable.

Different initialization schemes proposed in the literature are tested for case 1. Use of the scheme proposed by Gupta et al. [33] results in an unbounded feasible region for the RR solution, which prevents the algorithm from proceeding at the 1st iteration. With the K-value correlation developed by Zhu and Okuno [37], the algorithm successfully converges in 64 iterations.

The algorithm of Gupta et al. [33] is also tested for this case. It can be initialized if the K-value correlation of Zhu and Okuno [37] is used. However, it stops from proceeding at the 9th iteration due to an unbounded feasible region for the RR solution. Even if the RR issue is resolved by a proper modification, it still stops from proceeding at the 32nd iteration due to narrow-boiling behavior. This is because narrow-boiling behavior causes the system of equations to be nearly degenerate; thus, the decoupling of the variables should be performed as in this research. Their algorithm may also fail to converge to the correct solution because the number of phases can only decrease during the iteration with their algorithm.

One of the advantages of the new algorithm is that N_S gives the flexibility in terms of robustness and efficiency. It becomes more robust with increasing N_S at the expense of computational efficiency. As N_S increases, the algorithm become more robust because the possibility of finding all stationary points of the tangent-plane distance function increases. In case 1, the number of stationary points detected upon convergence is 3 with N_S of 3, 4 with N_S of 4 and 5, and 5 with N_S of 6 and higher. Fig. 5 shows the number of iterations required when starting with different N_S. All calculations start at the same initial T at 375 K. The three sampling points that are always used are near the compositional vertices. The other sampling compositions are randomly distributed for $N_S > 3$. The proposed algorithm successfully converges to the correct solution as long as N_S is greater than two. The number of iterations required tends to increase with increasing N_S because the algorithm with more sampling compositions may take more iterations when merging and adding some of the sampling compositions. This is a common observation for all the cases tested in this research.

The required number of iterations is 41 with the three sampling compositions placed near the compositional vertices. Interestingly,

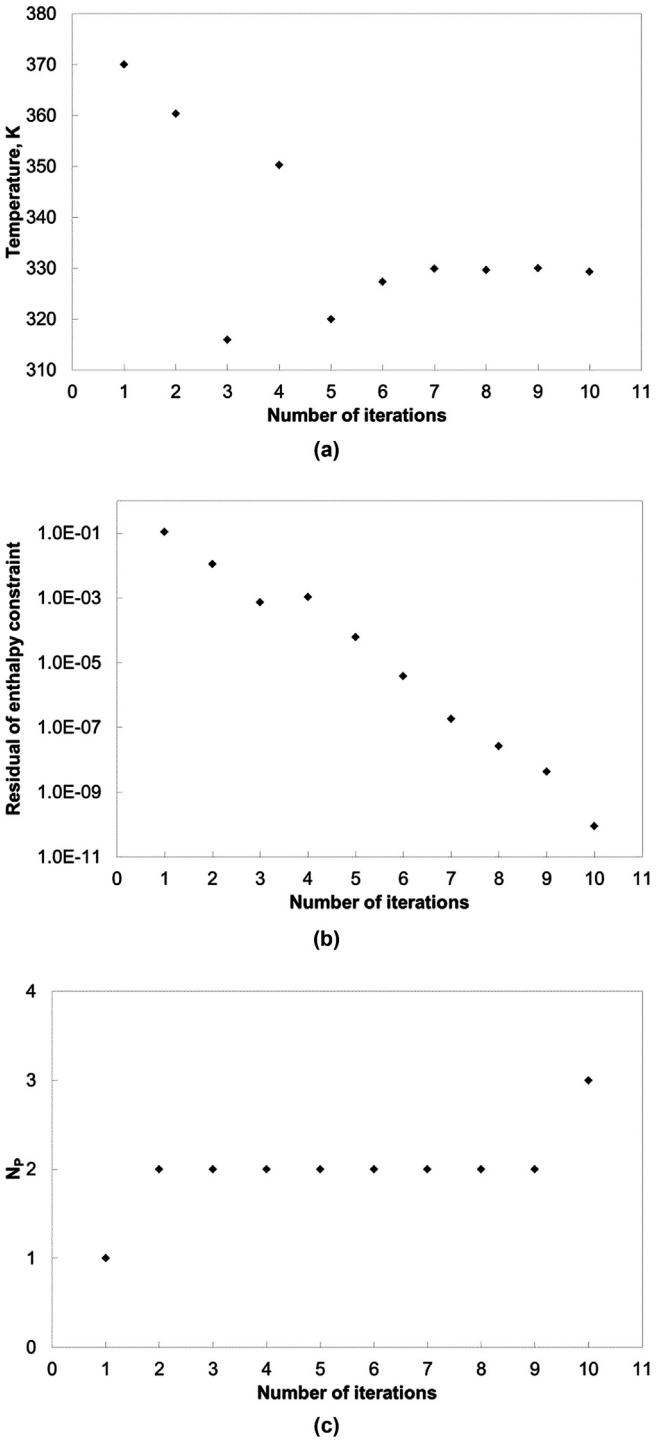

Fig. 10. Convergence behavior of the multiphase isenthalpic flash algorithm integrated with stability analysis at 10 bars and −42,925.99 J/mol for 99% water and 1% BSB oil: (a) T, (b) residual of equation 4, and (c) N_P. The components' properties are given in Table 3. The initial temperature is set to 370 K, which is in the V + W region. In this calculation, N_S is set to three. Two of the three sampling compositions are near vertices. The third is placed at the middle of the composition space. The solution temperature is 329.31 K, at which $\underline{H}^t$ is discontinuous with respect to temperature (see Fig. 8). The convergence is achieved at the 10th iteration.

this is much lower than the number of iterations, 64, required when the K-value correlation by Zhu and Okuno [37] is used, although the number of sampling points is the same for the two cases. This indicates that a physically-derived correlation for K values does not necessarily result in fewer iterations than a random distribution

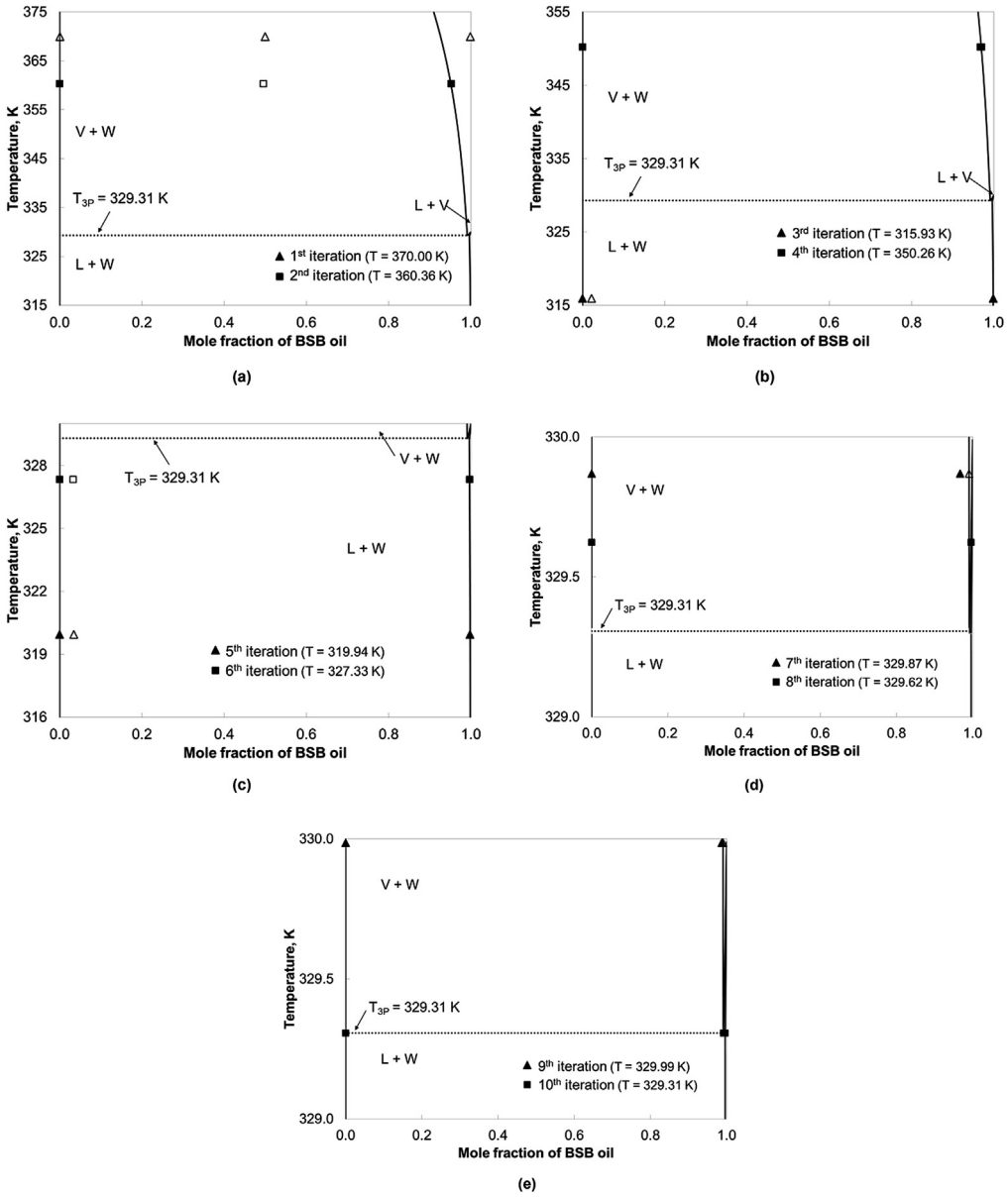

Fig. 11. T-x diagrams at 10 bars for 99% water and 1% BSB oil at different iteration steps during the solution: (a) the 1st and 2nd iterations, (b) the 3rd and 4th iterations, (c) the 5th and 6th iterations, (d) the 7th and 8th iterations, and (e) the 9th and 10th iterations. The components' properties are given in Table 3. In these figures, solid symbols represent the sampling compositions in set P, which are included in material balance. Hollow symbols represent the sampling compositions in set U. At the 1st iteration, all three sampling points are excluded from material balance due to the positive θ's. From the 2nd iteration to 9th iteration, the iterative temperatures switch between the L + W and V + W regions.

and a distribution near vertices in composition space with the algorithm developed.

The algorithm is further tested for 350 discrete PH specifications for the mixture given in Table 1. Fig. 6 shows the Jacobian condition number with respect to the number of iterations required. Among them, 240 PH conditions lie in a narrow-boiling region. All calculations start from the same initial T, 375 K, and three sampling compositions near the compositional vertices. Results show that the number of iterations required increases with the condition number of Jacobian matrix. Similar trends are observed for Cases 2 and 3, although not shown in this paper.

Table 4
Compositions of the three sampling points at the 10th iteration used for case 2.

	Composition 1	Composition 2	Composition 3
x_{ij}	$3.937372916 \times 10^{-3}$	$8.801870733 \times 10^{-3}$	$9.999999999 \times 10^{-1}$
	$9.960626270 \times 10^{-1}$	$9.911981292 \times 10^{-1}$	$1.380325011 \times 10^{-11}$

4.2. Case 2

Case 2 uses a binary mixture consisting of 99% water (w) and 1% Bob Slaughter Block (BSB) oil. The components' properties are given in Table 3. The four components used for the BSB oil by Okuno et al. [52] were grouped into one pseudo component by molar averaging. Note that the concentration of water is substantially higher than that of the pseudo component. Hence, this case is useful to show narrow-boiling behavior that occurs owing to the first condition mentioned in the preceding section, including a temperature point with one degree of freedom.

Fig. 7 presents the T-x cross section for this binary at 10 bars on the basis of the PR EOS. Three equilibrium phases, L, V, and W, are calculated to coexist at 329.31 K (T_{3P}). A discontinuity of two-phase K values occurs at T_{3P}. Also, K values in the V + W region rapidly change with temperature. This K-value behavior results in narrow-boiling behavior as shown in Fig. 8, which shows $\underline{H}^t$ from 300 K to

Table 5
Properties of the quaternary mixture (case 3).

Component	Mole fraction	MW g/mol	T_C K	P_C bar	ω	C^0_{P1} J/(mol·K)	C^0_{P2} J/(mol·K^2)	C^0_{P3} J/(mol·K^3)	C^0_{P4} J/(mol·K^4)
Water	0.75	18.015	647.3	220.89	0.344	32.20	1.907×10^{-3}	1.055×10^{-5}	-3.596×10^{-9}
C_1	0.08	16.043	190.6	46.00	0.008	19.30	5.212×10^{-2}	1.197×10^{-5}	-1.132×10^{-8}
C_7	0.15	100.205	540.2	27.36	0.351	−5.15	6.761×10^{-1}	-3.651×10^{-4}	7.657×10^{-8}
C_{GB}	0.02	594.600	1090.9	7.86	1.361	−34.60	3.801	-2.152×10^{-3}	0.000

Binary interaction parameters:

	Water	C_1	C_7	C_{GB}
Water	0.0000	0.7560	0.5610	0.1000
C_1	0.7560	0.0000	0.0352	0.0000
C_7	0.5610	0.0352	0.0000	0.0000
C_{GB}	0.1000	0.0000	0.0000	0.0000

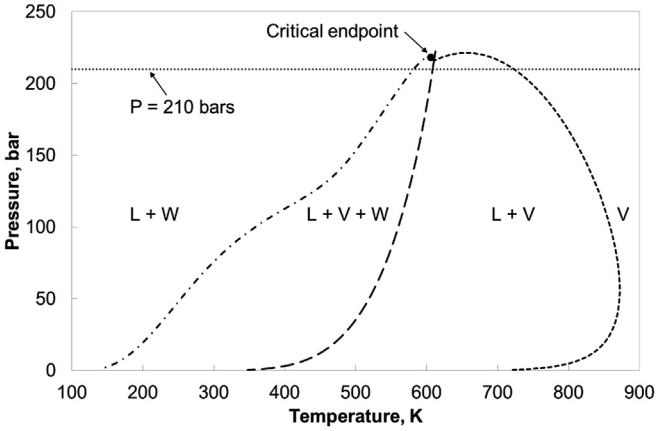

Fig. 12. P-T diagram for the quaternary mixture given in Table 5. The critical endpoint of type L = V + W is calculated at 605.73 K and 218.12 bars on the basis of the PR EOS. At 210 bars (near the critical endpoint), three phases (L + V + W) exist from 581.81 K to 608.52 K.

475 K at 10 bars. $\underline{H}^t$ is substantially nonlinear with respect to temperature. It is discontinuous at T_{3P}.

Fig. 9 presents the condition number of the Jacobian matrix and the Hessian of the RR convex function (equation (13)) within the V + W region at 10 bars. Note that the Hessian matrix for two-phase RR is of 1 × 1 (i.e., a scalar). T_{ref} of 300 K and $\underline{H}_{spec}$ of −5000 J/mol are used to calculate T_D and $\underline{H}^t_D$. Narrow-boiling behavior occurs for temperature above 447.73 K using the criterion that the condition number of the Jacobian matrix with dimensionless variables is greater than 10^6. It is evident from the figure that the convexity of the

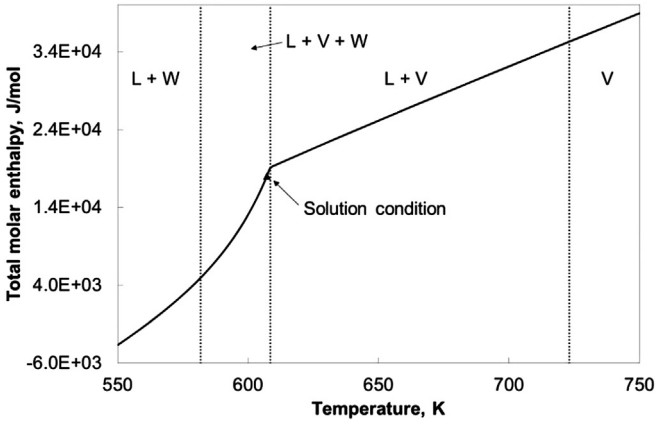

Fig. 13. Total molar enthalpy at 210 bars for the quaternary mixture given in Table 5. $\underline{H}^t$ at 210 bars is sensitive to temperature near the phase boundary between L + V + W and L + V, where three-phase PH flash is challenging.

RR convex function is substantially reduced in the narrow-boiling region, which verifies the analysis given in the previous section.

A PH flash calculation at 10 bars and −42,925.99 J/mol is considered for this binary mixture. The initial temperature is set to 370 K, which is in the V + W region. In this calculation, N_S is set to three. Two of the three sampling compositions are near vertices. The third is placed at the middle of the composition space, to be uniform in distributing three sampling compositions. The solution temperature is 329.31 K, at which $\underline{H}^t$ is discontinuous with respect to temperature (see Fig. 8). Fig. 10 shows the convergence behavior of the algorithm in terms of T, residual of equation (4) (g_{NP}), and N_P. The algorithm only uses Newton's iteration steps without decoupling the system of equations. This is because narrow-boiling behavior does not occur in the vicinity of the solution temperature, as can be seen in Fig. 8. The convergence is achieved at the 10th iteration. Unlike prior algorithms (e.g., Agarwal et al. [32], Michelsen [34], and Zhu and Okuno [37]), the new algorithm does not have to detect any temperature oscillation, and directly solve for one degree of freedom.

Fig. 11 shows the three sampling compositions at different iteration steps during the solution. In these figures, solid symbols represent the sampling compositions in set P, which are included in material balance. Hollow symbols represent the sampling compositions in set U. At the 1st iteration, all three sampling points are excluded from material balance due to the positive θ's. From the 2nd iteration to 9th iteration, the iterative temperatures switch

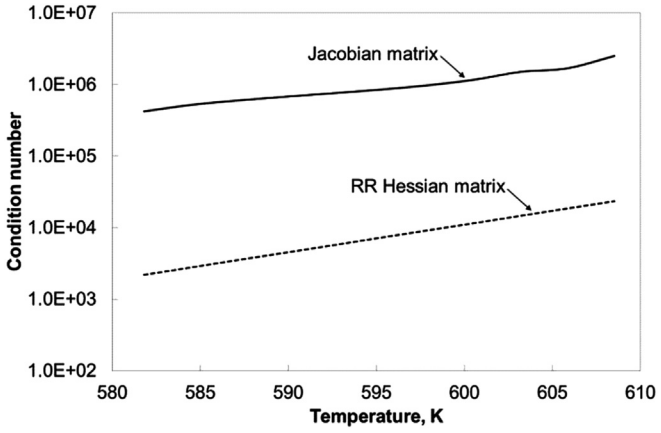

Fig. 14. Condition numbers of the Jacobian matrix and the RR Hessian matrix within the three-phase region at 210 bars for the quaternary mixture given in Table 5. Temperature and enthalpy are made dimensionless with T_{ref} of 300 K and $\underline{H}_{spec}$ of 18,000 J/mol. Narrow-boiling behavior occurs for temperatures above 598.32 K based on the criterion that the condition number of the Jacobian with dimensionless variables is greater than 10^6. The Jacobian matrix is more ill-conditioned as the convexity level of the RR convex function becomes lower.

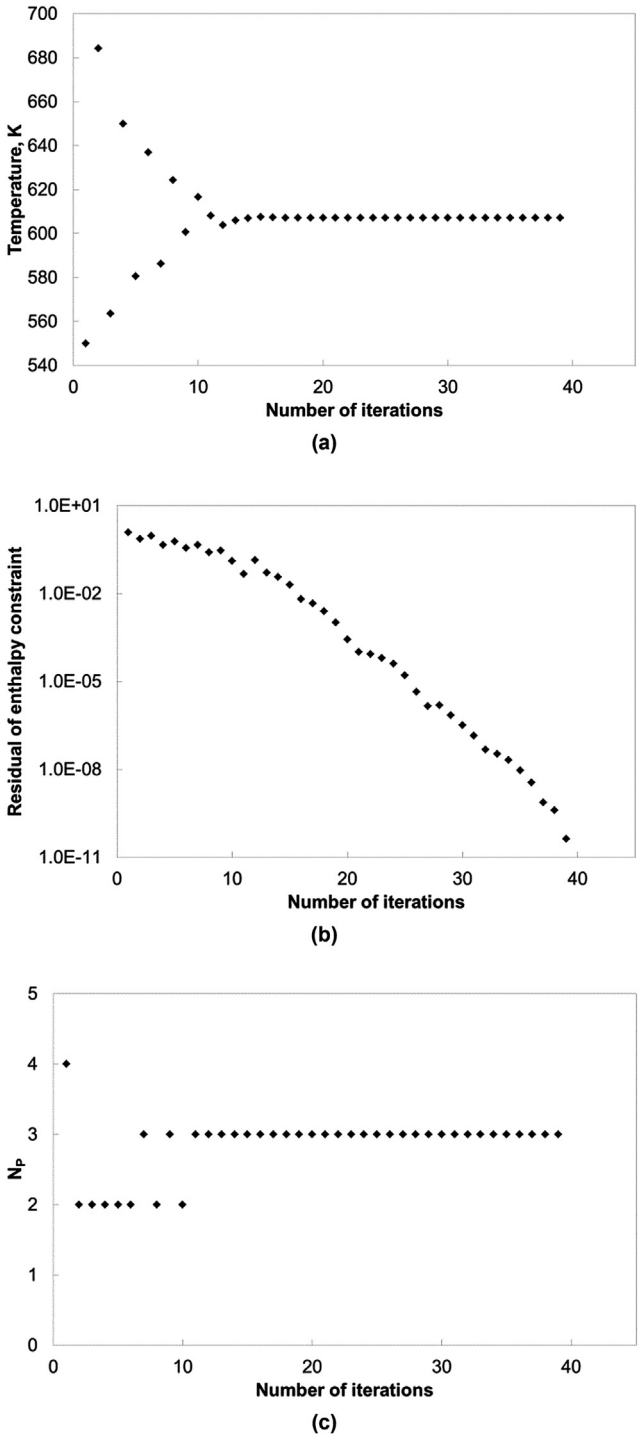

Fig. 15. Convergence behavior of the current algorithm for the quaternary mixture given in Table 5 at 210 bars and 18,000 J/mol: (a) T, (b) residual of equation 4, and (c) N_P. The initial temperature is set to 550 K. Four initial sampling points are placed near the compositional vertices. The solution temperature is 607.17 K, which is in the region of narrow-boiling behavior (see Fig. 13). T_D is decoupled from β's from the 9th iteration until the convergence is achieved at the 39th iteration.

between the L + W and V + W regions. The final set of sampling compositions for three equilibrium phases is shown in Table 4.

4.3. Case 3

Case 3 uses a quaternary mixture consisting of 75% water (w), 8% C_1, 15% n-C_7 (C_7), and 2% Athabasca (GCOS) bitumen (C_{GB}). Johnson [53] developed a four-pseudo-component model for this bitumen. Mehrotra and Svrcek [54] presented a single pseudo component for the bitumen based on the four-pseudo-component model of Johnson [53]. Properties used for this mixture are given in Table 5. The composition is located well inside multicomponent composition space. Case 3 shows narrow-boiling behavior that occurs near a critical endpoint.

Fig. 12 presents the P-T diagram calculated for the mixture by using the PR EOS. A critical endpoint of type L = V + W is calculated at 605.73 K and 218.12 bars. At 210 bars (near the critical endpoint), three phases (L + V + W) exist from 581.81 K to 608.52 K. Fig. 13 shows that $\underline{H}^t$ at 210 bars is sensitive to temperature near the phase boundary between L + V + W and L + V, where three-phase PH flash is challenging. Fig. 14 presents the condition numbers of the Jacobian matrix and the RR Hessian matrix within the three-phase region at 210 bars. Temperature and enthalpy are made dimensionless with T_{ref} of 300 K and $\underline{H}_{spec}$ of 18,000 J/mol. Narrow-boiling behavior occurs for temperatures above 598.32 K based on the criterion that the condition number of the Jacobian with dimensionless variables is greater than 10^6. The Jacobian matrix is more ill-conditioned as the convexity level of the RR convex function becomes lower, which is in line with the analysis given in the previous section.

A PH flash calculation at 210 bars and 18,000 J/mol is considered for this quaternary mixture. The initial temperature is set to 550 K. Four initial sampling points are placed near the compositional vertices. The solution temperature is 607.17 K, which is in the region of narrow-boiling behavior (see Fig. 13). T_D is decoupled from β's from the 9th iteration until the convergence is achieved at the 39th iteration. Fig. 15 shows the iterative solution in terms of T, residual of equation (4) (g_{NP}), and N_P. Sampling points does not merge in this case. N_P and, therefore, N_U change quite often in the early stage of the iterative solution. Fig. 15b and c shows that the convergence becomes more rapid after N_P becomes stable at the correct number of phases, which is three in this case. The final set of sampling compositions is given in Table 6. The three equilibrium phases are compositions 2, 3, and 4. The other composition has a positive θ value of 0.1689; i.e., the tangent plane distance at that composition.

5. Conclusions

This paper presented a new algorithm for multiphase PH flash integrated with stability analysis. The correct set of equations is solved for stationary points on the tangent-plane-distance function that is defined at an adaptively selected reference composition. This paper also presented an analysis of narrow-boiling behavior on the basis of the multiphase PH-flash equations, where energy and phase behavior equations are coupled through the temperature dependency of K values. Case studies were presented to demonstrate the robustness of the new algorithm and the narrow-boiling conditions derived in this research. Conclusions are as follows:

1. The new algorithm can robustly solve PH flash for narrow-boiling fluids. It does not require a special treatment for one degree of freedom, for which the total enthalpy is discontinuous in temperature. This is because the algorithm does not require to fix the number of equilibrium phases in the iteration. The advantage of the proposed algorithm is pronounced when the fluid of interest exhibits complex phase appearance/disappearance, and/or when narrow-boiling behavior is involved, as in thermal compositional flow simulation.
2. The initialization of PH flash is possible even when no reliable information is available about the equilibrium phases of the fluid of interest. In this research, sampling compositions were

Table 6
Compositions of the four sampling points at the 39th iteration (case 3).

	Composition 1	Composition 2	Composition 3	Composition 4
x_{ij}	$4.197334218 \times 10^{-1}$	$7.378538213 \times 10^{-1}$	$6.879222220 \times 10^{-1}$	$9.980050616 \times 10^{-1}$
	$1.843513051 \times 10^{-1}$	$9.476609831 \times 10^{-2}$	$7.622206172 \times 10^{-2}$	$1.976024256 \times 10^{-3}$
	$3.493368998 \times 10^{-1}$	$1.569487131 \times 10^{-1}$	$1.883863288 \times 10^{-1}$	$1.891409537 \times 10^{-5}$
	$4.657837340 \times 10^{-2}$	$1.043136733 \times 10^{-2}$	$4.746938752 \times 10^{-2}$	$5.853975844 \times 10^{-13}$

placed near compositional vertices for such cases. Also, additional sampling compositions were randomly distributed in composition space. No K-value correlation is necessary to initialize the new algorithm.

3. The algorithm offers the flexibility in terms of robustness and efficiency depending on the number of sampling compositions (N_S) used. It becomes more robust with increasing N_S at the expense of computational efficiency. As N_S increases, the algorithm become more robust because the possibility of finding all stationary points of the tangent-plane distance function increases. However, the number of iterations required tends to increase with increasing N_S because the algorithm with more sampling compositions may take more iterations when merging and adding some of the sampling compositions.
4. The algorithm presented in this paper is substantially different from that of Gupta et al. [33]. An important difference comes from the difference in formulation; that is, they introduced an additional set of equations that was called “stability equations” in their paper. However, this research clearly showed that the complete formulation does not require Gupta et al.’s stability equations. Consequently, the Jacobian matrix in the new algorithm is always smaller than that of Gupta et al.
5. The general condition for narrow-boiling behavior is that the interplay between the energy and phase behavior equations is significant. Two subsets of the narrow-boiling condition were derived by analyzing the convex function whose gradient vectors consist of the RR equations; (i) the overall composition is near an edge of composition space, and (ii) the solution conditions (temperature, pressure, and overall composition) are near a critical point, including a critical endpoint. A special case of the first specific condition is the fluids with one degree of freedom, for which enthalpy is discontinuous in temperature space.
6. The analysis of the RR convex function gave the clear limiting conditions toward which the tendency of narrow-boiling behavior increases. Narrow-boiling behavior tends to occur in thermal compositional simulation likely because water is by far the most dominant component in the fluid systems formed in the simulation.

Acknowledgments

This research was funded by research grants from the Natural Sciences and Engineering Research Council of Canada (RGPIN 418266), Japan Petroleum Exploration Co., Ltd. (JAPEX), and Japan Canada Oil Sands Ltd. (JACOS). Di Zhu also received financial support from the China Scholarship Council. We gratefully acknowledge these supports. Section 3 of this paper was presented at the 2015 SPE Reservoir Simulation Symposium, 23–25 February, Houston, Texas, U.S.A.

Nomenclature

Roman Symbols

a	Parameter defined in equation 14
b	Parameter defined in equation 14
D	Diagonal matrix defined in equation 15
F	Non-monotonic convex function defined in equation 13
f_{ij}	Unified tangent-plane-distance equations define in equation 8
g_j	Material-balance equations [for $j = 1, 2, \ldots, (N_P - 1)$] defined in equation 10
g_{NP}	Enthalpy equation defined in equation 4
H	Enthalpy or the Hessian matrix defined in equation 15
$\underline{H}$	Molar enthalpy
K_{ij}	K value of component i in phase j
L_1	Oleic-rich liquid phase
L_2	Solvent-rich liquid phase
N_C	Number of components
N_P	Number of sampling points that are included in material-balance equations
N_S	Number of sampling points
N_U	Number of sampling points that are excluded from material-balance equations
P	Pressure
$\underline{S}$	Molar entropy
t_i	Parameter defined in equation 10
T	Temperature
V	Vapor phase
W	Aqueous phase
x_{ij}	Mole fraction of component i in phase j
Y	Symmetric matrix defined in equation 15
z_i	Mole fraction of component i in a mixture

Greek Symbols

β_j	Mole fraction of phase j
$\boldsymbol{\beta}$	Vector of independent mole fractions β_j for $j = 1, 2, \ldots, (N_P - 1)$ used in equations (13) and (14)
θ_j	Stability variable of phase j as calculated by equation 11
φ_{ij}	Fugacity coefficient of component i in phase j
ε	Convergence criterion

Subscripts

D	Dimensionless property
i	Component index
j	Phase index
L	Lower limit
r/Ref	Reference value
spec	Specified value
U	Upper limit
w	Water component

Superscripts

k	Iteration-step number
t	Total property
T	Transpose

Abbreviations

BIP	Binary interaction parameter
BSB	Bob Slaughter Block
C_B	Bitumen
C_{GB}	Athabasca (GCOS) dead bitumen
D	Tangent plane distance function
DS	Direct substitution

EOS Equation of state
PH Isobaric isenthalpic
PR Peng-Robinson
PT Isobaric isothermal
RR Rachford-Rice

Appendix A. Flow chart of the multiphase isenthalpic flash algorithm integrated with stability analysis

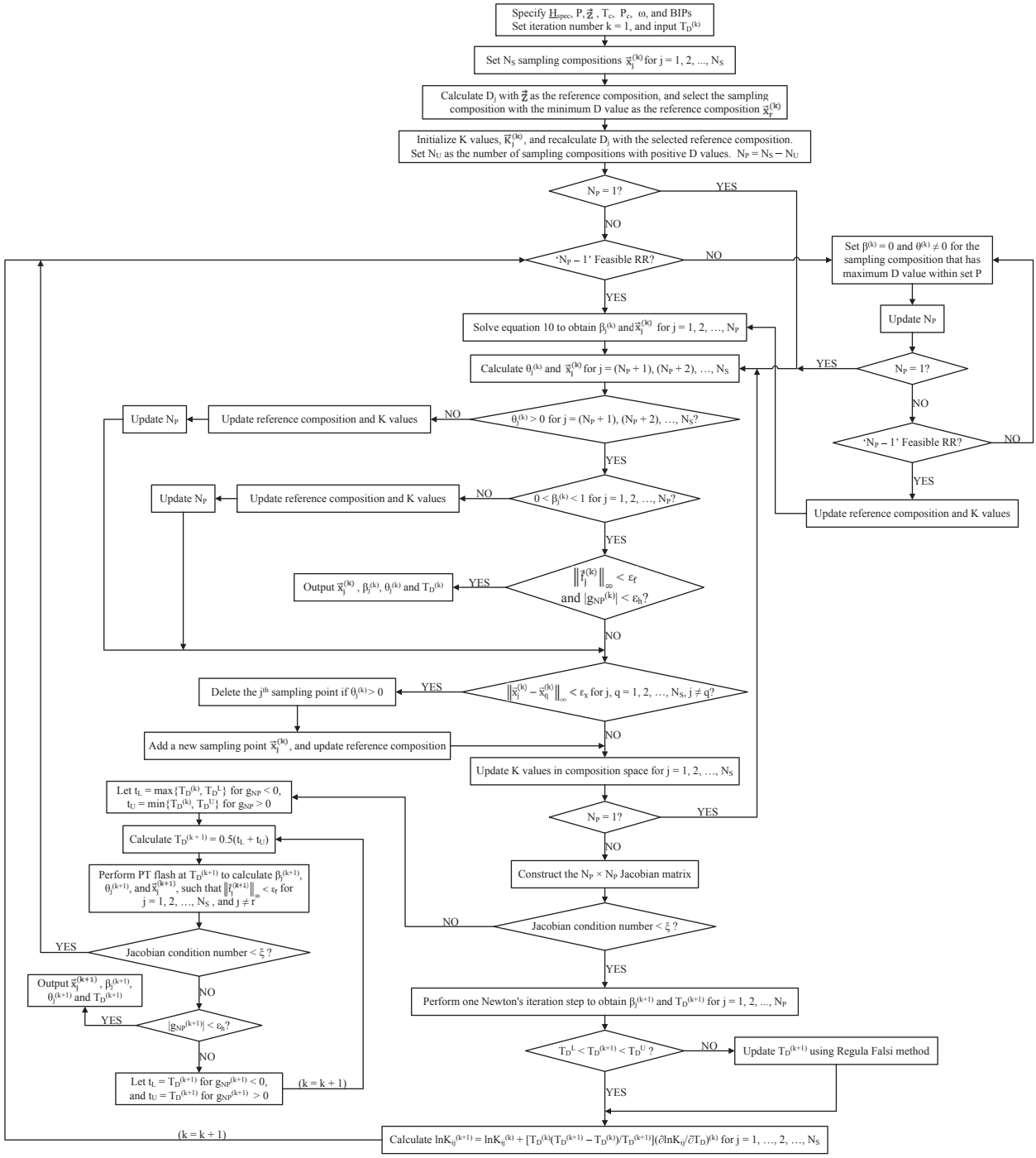

Appendix B. Jacobian matrix and analysis of the system of equations

Appendix B-1. Jacobian matrix

The elements of the Jacobian matrix used in the proposed algorithm for a N_C-component N_P-phase system are

$$\frac{\partial g_j}{\partial T_D} = -T_{ref}\sum_{i=1}^{N_C}\frac{z_i}{t_i^2}\left[t_i K_{ij}\frac{\partial \ln K_{ij}}{\partial T} - (K_{ij}-1)\sum_{k=1}^{N_P-1}\beta_k K_{ik}\frac{\partial \ln K_{ik}}{\partial T}\right] \text{ for } j = 1, 2, \cdots, N_P-1, \tag{B-1}$$

$$\frac{\partial g_j}{\partial \beta_k} = \sum_{i=1}^{N_C}\frac{z_i}{t_i^2}(1-K_{ij})(1-K_{ik}) \text{ for } j,\ k = 1, 2, \cdots, N_P-1, \tag{B-2}$$

$$\frac{\partial g_{N_P}}{\partial T_D} = T_{ref}\sum_{j=1}^{N_P}\beta_j\left(\sum_{i=1}^{N_C}\frac{\partial x_{ij}}{\partial T}\frac{\underline{H}_i^{IG}}{\underline{H}_{spec}} + \sum_{i=1}^{N_C}\frac{x_{ij}}{\underline{H}_{spec}}\frac{\partial \underline{H}_i^{IG}}{\partial T} + \frac{\partial \underline{H}_{Dj}^{dep}}{\partial T}\right), \tag{B-3}$$

$$\frac{\partial g_{N_P}}{\partial \beta_k} = \left(\underline{H}_{Dk}^{IGM} + \underline{H}_{Dk}^{dep}\right) - \left(\underline{H}_{DN_P}^{IGM} + \underline{H}_{DN_P}^{dep}\right) \text{ for } k = 1, 2, \cdots, N_P-1, \tag{B-4}$$

where $t_i = 1 - \sum_{j=1}^{N_P-1}(1-K_{ij})\beta_j$ for $i = 1, 2, \ldots, N_C$, $g_j = \sum_{i=1}^{N_C}(1-K_{ij})z_i/t_i = 0$ for $j = 1, 2, \ldots, (N_P - 1)$, and $g_{NP} = (\underline{H}^t - \underline{H}_{spec})/\underline{H}_{spec} = 0$. Pertinent derivatives used can be found in Zhu and Okuno [36].

Appendix B-2. Analysis of the system of equations

The Jacobian matrix of $N_P \times N_P$ can be written as follows:

$$J = \begin{bmatrix} \frac{\partial g_{N_P}}{\partial T_D} & \frac{\partial g_{N_P}}{\partial \beta_1} & \cdots & \frac{\partial g_{N_P}}{\partial \beta_{N_P-1}} \\ \frac{\partial g_1}{\partial T_D} & \frac{\partial g_1}{\partial \beta_1} & \cdots & \frac{\partial g_1}{\partial \beta_{N_P-1}} \\ \vdots & \vdots & \ddots & \vdots \\ \frac{\partial g_{N_P-1}}{\partial T_D} & \frac{\partial g_{N_P-1}}{\partial \beta_1} & \cdots & \frac{\partial g_{N_P-1}}{\partial \beta_{N_P-1}} \end{bmatrix} = \begin{bmatrix} J_{11} & J_{12} & \cdots & J_{1N_P} \\ J_{21} & J_{22} & \cdots & J_{2N_P} \\ \vdots & \vdots & \ddots & \vdots \\ J_{N_P1} & J_{N_P2} & \cdots & J_{N_PN_P} \end{bmatrix} = \begin{bmatrix} J_{11} & P^{1\times(N_P-1)} \\ Q^{(N_P-1)\times 1} & R^{(N_P-1)\times(N_P-1)} \end{bmatrix}, \tag{B-5}$$

where J_{11} is equation B-3, $Q^{(N_P-1)\times 1}$ consists of equations B-1, $P^{1\times(N_P-1)}$ consists of equations B-4, and $R^{(N_P-1)\times(N_P-1)}$ is the Hessian matrix of F consisting of equations B-2.

Gaussian elimination for $Q^{(N_P-1)\times 1}$ yields

$$J' = \begin{bmatrix} J_{11} & P^{1\times(N_P-1)} \\ 0^{(N_P-1)\times 1} & R'^{(N_P-1)\times(N_P-1)} \end{bmatrix}, \text{ where } R' = \frac{1}{J_{11}}\begin{bmatrix} J_{22}J_{11} - J_{12}J_{21} & \cdots & J_{2N_P}J_{11} - J_{1N_P}J_{21} \\ \vdots & \ddots & \vdots \\ J_{2N_P}J_{11} - J_{12}J_{N_P1} & \cdots & J_{N_PN_P}J_{11} - J_{1N_P}J_{N_P1} \end{bmatrix} \tag{B-6}$$

Equation B-6 clearly indicates that the system of equations tend to be degenerate with increasing J_{11}, regardless of the curvature of the RR convex function.

Also, matrix J is singular, when R is not of full rank. To see this, consider matrix J when the pth and qth phases are critical ($p \neq q$). As described in Okuno et al. [9], $J_{mp} = J_{mq}$, where $m = 2, 3, \ldots, N_P$, for such a case. $J_{1p} = J_{1q}$ when the compositions of the two phases are identical. Therefore, the pth and qth columns of matrix J are identical when R is not of full rank.

References

[1] A. Belkadi, W. Yan, E. Moggia, M.L. Michelsen, E.H. Stenby, I. Aavatsmark, E. Vignati, A. Cominelli, Speeding up Compositional Reservoir Simulation through an Efficient Implementation of Phase Equilibrium Calculation, Paper SPE-163598-MS presented at the SPE Reservoir Simulation Symposium, February 18–20, the Woodlands, Texas, 2013, http://dx.doi.org/10.2118/163598-MS.

[2] Y.-B. Chang, Development and Application of an Equation of State Compositional Simulator, PhD dissertation, the University of Texas at Austin, Austin, Texas, 1990.

[3] Y.-B. Chang, G.A. Pope, K. Sepehrnoori, A higher-order finite-difference compositional simulator, J. Pet. Sci. Eng. 5 (1) (1990) 35–50. http://dx.doi.org/10.1016/0920-4105(90)90004-M.

[4] A. Iranshahr, D.V. Voskov, H.A. Tchelepi, A negative-flash tie-simplex approach for multiphase reservoir simulation, SPE J. 18 (6) (2013) 1140–1149. SPE-141896-PA, http://dx.doi.org/10.2118/141896-PA.

[5] S.A. Khan, An Expert System to Aid in Compositional Simulation of Miscible Gas Flooding, PhD dissertation, the University of Texas at Austin, Austin, Texas, 1992.

[6] R.K. Mehra, R.A. Heidemann, K. Aziz, Computation of multiphase equilibrium for compositional simulation, SPE J. 22 (1) (1982) 61–68. SPE-9232-PA, http://dx.doi.org/10.2118/9232-PA.

[7] S. Mohebbinia, Advanced Equation of State Modeling for Compositional Simulation of Gas Floods, PhD dissertation, the University of Texas at Austin, Austin, Texas, 2013.

[8] R. Okuno, R.T. Johns, K. Sepehrnoori, Application of a reduced method in compositional simulation, SPE J. 15 (1) (2010a) 39–49. SPE-119657-PA, http://dx.doi.org/10.2118/119657-PA.

[9] R. Okuno, R.T. Johns, K. Sepehrnoori, A new algorithm for Rachford-Rice for multiphase compositional simulation, SPE J. 15 (2) (2010b) 313–325. SPE-117752-PA, http://dx.doi.org/10.2118/117752-PA.

[10] R. Okuno, R.T. Johns, K. Sepehrnoori, Three-phase flash in compositional simulation using a reduced method, SPE J. 15 (3) (2010c) 689–703. SPE-125226-PA, http://dx.doi.org/10.2118/125226-PA.

[11] H. Pan, H.A. Tchelepi, Compositional Flow Simulation Using Reduced-variables and Stability-analysis Bypassing, Paper SPE-142189-MS presented at the SPE Reservoir Simulation Symposium. February 21–23, the Woodlands, Texas, 2011, http://dx.doi.org/10.2118/142189-MS.

[12] D.R. Perschke, Equation of State Phase Behavior Modeling for Compositional Simulation, PhD dissertation, the University of Texas at Austin, Austin, Texas, 1988.

[13] D.R. Perschke, Y.-B. Chang, G.A. Pope, K. Sepehrnoori, Comparison of Phase Behavior Algorithms for an Equation-of-state Compositional Simulator, Paper SPE-19443-MS available from SPE, Richardson, Texas, 1989.

[14] M. Rezaveisi, K. Sepehrnoori, R.T. Johns, Tie-simplex-based phase-behavior modeling in an IMPEC reservoir simulator, SPE J. 19 (2) (2014) 327–339. SPE-163676-PA, http://dx.doi.org/10.2118/163676-PA.

[15] J.A. Trangenstein, Minimization of Gibbs Free Energy in Compositional Reservoir Simulation, Paper SPE-13520-MS presented at the SPE Reservoir Simulation Symposium, February 10–13, Dallas, Texas, 1985, http://dx.doi.org/10.2118/13520-MS.

[16] J.A. Trangenstein, Customized minimization techniques for phase equilibrium computations in reservoir simulation, Chem. Eng. Sci. 42 (12) (1987) 2847–2863. http://dx.doi.org/10.1016/0009-2509(87)87051-3.

[17] J.A. Trangenstein, J.B. Bell, Mathematical structure of compositional reservoir simulation, SIAM J. Sci. Stat. Comput. 10 (5) (1989) 817–845. http://dx.doi.org/10.1137/0910049.

[18] P. Wang, E.H. Stenby, Non-iterative flash calculation algorithm in compositional reservoir simulation, Fluid Ph. Equilib. 94 (1994) 93–108. http://dx.doi.org/10.1016/0378-3812(94)80063-4.

[19] P. Wang, J.W. Barker, Comparison of Flash Calculations in Compositional Reservoir Simulation, Paper SPE-30787-MS presented at the SPE Annual Technical Conference and Exhibition, October 22–25, Dallas, Texas, 1995, http://dx.doi.org/10.2118/30787-MS.

[20] R. Zaydullin, D. Voskov, H.A. Tchelepi, Nonlinear formulation based on an equation-of-state free method for compositional flow simulation, SPE J. 18 (2) (2012) 264–273. SPE-146989-PA, http://dx.doi.org/10.2118/146989-PA.

[21] K.M. Brantferger, Development of a Thermodynamically Consistent, Fully Implicit, Compositional, Equation-of-state, Steamflood Simulator, PhD dissertation, the University of Texas at Austin, Austin, Texas, 1991.

[22] M.C.H. Chien, H.E. Yardumian, E.Y. Chung, W.W. Todd, The Formulation of a Thermal Simulation Model in a Vectorized, General Purpose Reservoir Simulator, Paper SPE-18418-MS presented at the SPE Symposium on Reservoir Simulation, February 6–8, Houston, Texas, 1989, http://dx.doi.org/10.2118/18418-MS.
[23] J.W. Grabowski, P.K. Vinsome, R.C. Lin, G.A. Behie, B. Rubin, A Fully Implicit General Purpose Finite-difference Thermal Model for in Situ Combustion and Steam, Paper SPE-8396-MS presented at the SPE Annual Technical Conference and Exhibition, September 23–26, Las Vegas, Nevada, 1979, http://dx.doi.org/10.2118/8396-MS.
[24] M. Heidari, L.X. Nghiem, B.B. Maini, Improved Isenthalpic Multiphase Flash Calculations for Thermal Compositional Simulators, Paper SPE-170029-MS presented at the SPE Heavy Oil Conference-Canada, June 10–12, Calgary, Alberta, Canada, 2014, http://dx.doi.org/10.2118/170029-MS.
[25] A. Iranshahr, D.V. Voskov, H.A. Tchelepi, Tie-simplex parameterization for EOS-based thermal compositional simulation, SPE J. 15 (2) (2010) 545–556. SPE-119166-PA, http://dx.doi.org/10.2118/119166-PA.
[26] K. Ishimoto, G.A. Pope, K. Sepehrnoori, An equation of state steam simulator, In Situ 11 (1) (1987) 1–37.
[27] K. Liu, G. Subramanian, D.I. Dratler, J.P. Lebel, J.A. Yerian, A general unstructured-grid, equation-of-state-based, fully implicit thermal simulator for complex reservoir processes, SPE J. 14 (2) (2009) 355–361. SPE-106073-PA, http://dx.doi.org/10.2118/106073-PA.
[28] B. Rubin, W.L. Buchanan, A general purpose thermal model, SPE J. 25 (2) (1985) 202–214. SPE-11713-PA, http://dx.doi.org/10.2118/11713-PA.
[29] A.L. Siu, B.J. Rozon, Y.K. Li, L.X. Nghiem, W.H. Acteson, M.E. McCormack, A fully implicit thermal Wellbore model for multicomponent fluid flows, SPE Reserv. Eng. 6 (3) (1991) 302–310. SPE-18777-PA, http://dx.doi.org/10.2118/18777-PA.
[30] A. Varavei, K. Sepehrnoori, An EOS-based Compositional Thermal Reservoir Simulator, Paper SPE-119154-MS presented at the SPE Reservoir Simulation Symposium, February 2–4, The Woodlands, Texas, 2009, http://dx.doi.org/10.2118/119154-MS.
[31] R. Zaydullin, D.V. Voskov, S.C. James, H. Henley, A. Lucia, Fully compositional and thermal reservoir simulation, Comput. Chem. Eng. 63 (2014) 51–65. http://dx.doi.org/10.1016/j.compchemeng.2013.12.008.
[32] R.K. Agarwal, Y.K. Li, L.X. Nghiem, D.A. Coombe, Multiphase multicomponent isenthalpic flash calculations, J. Can. Pet. Technol. 30 (3) (1991) 69–75. PETSOC-91-03-07, http://dx.doi.org/10.2118/91-03-07.
[33] A.K. Gupta, P.R. Bishnoi, N. Kalogerakis, Simultaneous multiphase isothermal/isenthalpic flash and stability calculations for reacting/non-reacting systems, Gas Sep. Purif. 4 (1990) 215–222. http://dx.doi.org/10.1016/0950-4214(90)80045-M.
[34] M.L. Michelsen, Multiphase isenthalpic and isentropic flash algorithms, Fluid Ph. Equilib. 33 (1–2) (1987) 13–27. http://dx.doi.org/10.1016/0378-3812(87)87002-4.
[35] M.L. Michelsen, State function based flash specifications, Fluid Ph. Equilib. 158–160 (1999) 617–626. http://dx.doi.org/10.1016/S0378-3812(99)00092-8.
[36] D. Zhu, R. Okuno, A robust algorithm for isenthalpic flash of narrow-boiling fluids, Fluid Ph. Equilib. 379 (2014a) 26–51. http://dx.doi.org/10.1016/j.fluid.2014.07.003.
[37] D. Zhu, R. Okuno, Robust isenthalpic flash for multiphase water/hydrocarbon mixtures, SPE J. 20 (6) (2014b) 1350–1365. SPE-170092-PA, http://dx.doi.org/10.2118/170092-PA.
[38] K.M. Brantferger, G.A. Pope, K. Sepehrnoori, Development of a Thermodynamically Consistent, Fully Implicit, Equation-of-state, Compositional Steamflood Simulator, Paper SPE-21253-MS presented at the SPE Symposium on Reservoir Simulation, February 17–20, Anaheim, California, 1991, http://dx.doi.org/10.2118/21253-MS.
[39] J. Gernert, A. Jäger, R. Span, Calculation of phase equilibria for multi-component mixtures using highly accurate Helmholtz energy equations of state, Fluid Ph. Equilib. 375 (2014) 209–218. http://dx.doi.org/10.1016/j.fluid.2014.05.012.
[40] M.L. Michelsen, Phase equilibrium calculations. What is easy and what is difficult? Comput. Chem. Eng. 17 (5–6) (1993) 431–439. http://dx.doi.org/10.1016/0098-1354(93)80034-K.
[41] D.E.A. Van Odyck, J.B. Bell, F. Monmont, N. Nikiforakis, The mathematical structure of multiphase thermal models of flow in porous media, in: Proceedings of the Royal Society A: Mathematical, Physical and Engineering Science 465(2102), 2009, pp. 523–549. http://dx.doi.org/10.1137/0910049.
[42] N.M. Alsaifi, P. Englezos, Prediction of multiphase equilibrium using the PC-SAFT equation of state and simultaneous testing of phase stability, Fluid Ph. Equilib. 302 (1) (2011) 169–178. http://dx.doi.org/10.1016/j.fluid.2010.09.002.
[43] L.E. Baker, A.C. Pierce, K.D. Luks, Gibbs energy analysis of phase equilibria, SPE J. 22 (5) (1982) 731–742. SPE-9806-PA, http://dx.doi.org/10.2118/9806-PA.
[44] M.L. Michelsen, The isothermal flash problem. Part I, Stability Fluid Ph. Equilib. 9 (1) (1982) 1–19. http://dx.doi.org/10.1016/0378-3812(82)85001-2.
[45] Z. Li, A. Firoozabadi, General strategy for stability testing and phase-split calculation in two and three phases, SPE J. 17 (4) (2012) 1096–1107. SPE-129844-PA, http://dx.doi.org/10.2118/129844-PA.
[46] D.-Y. Peng, D.B. Robinson, A new two-constant equation of state, Ind. Eng. Chem. Fundam. 15 (1) (1976a) 59–64. http://dx.doi.org/10.1021/i160057a011.
[47] D.-Y. Peng, D.B. Robinson, Two and three phase equilibrium calculations for systems containing water, Can. J. Chem. Eng. 54 (5) (1976b) 595–599. http://dx.doi.org/10.1002/cjce.5450540620.
[48] D. Zhu, R. Okuno, Analysis of Narrow-boiling Behavior for Thermal Compositional Simulation, Paper SPE-173234-MS presented at the SPE Reservoir Simulation Symposium, 23–25 February, Houston, Texas, 2015, http://dx.doi.org/10.2118/173234-MS.
[49] M.L. Michelsen, Calculation of multiphase equilibrium, Comput. Chem. Eng. 18 (7) (1994) 545–550. http://dx.doi.org/10.1016/0098-1354(93)E0017-4.
[50] C.F. Leibovici, D.V. Nichita, A new look at multiphase Rachoford-Rice equations for negative flash, Fluid Ph. Equilib. 267 (2008) 127–132. http://dx.doi.org/10.1016/j.fluid.2008.03.006.
[51] A.V. Venkatramani, Modeling of Water-containing Reservoir Oil for Steam Injection Simulation, MSc thesis, the University of Alberta, Alberta, 2014.
[52] R. Okuno, R.T. Johns, K. Sepehrnoori, Mechanisms for high displacement efficiency of low-temperature CO_2 floods, SPE J. 16 (4) (2011) 751–767. SPE-129846-PA, http://dx.doi.org/10.2118/129846-PA.
[53] S.E. Johnson, Gas-Free and Gas-Saturated Bitumen Viscosity Prediction Using the Extended Principle of Corresponding State, MSc thesis, the University of Calgary, Calgary, Alberta, 1985.
[54] A.K. Mehrotra, W.Y. Svrcek, Corresponding state method for calculating Bitumen viscosity, J. Can. Pet. Technol. 26 (5) (1987) 60–66. PETSOC-87-05-06, http://dx.doi.org/10.2118/87-05-06.